สารป้องกันรังสียูวี-เอ และยูวี -บี สำหรับการรักษาโรคสะเก็ดเงินด้วยแสง

นางสาวสรวงสุดา มาเวหา

วิทยานิพนธ์นี้เป็นส่วนหนึ่งของการศึกษาตามหลักสูตรปริญญาวิทยาศาสตรมหาบัณฑิต
สาขาวิชาเทคโนโลยีชีวภาพ
คณะวิทยาศาสตร์ จุฬาลงกรณ์มหาวิทยาลัย
ปีการศึกษา 2560

UV-A AND -B BLOCKING AGENTS FOR PSORIASIS PHOTOTHERAPY

Miss Sruangsuda Mawaha

A Thesis Submitted in Partial Fulfillment of the Requirements
for the Degree of Master of Science Program in Biotechnology
Faculty of Science
Chulalongkorn University
Academic Year 2017

Thesis Title	UV-A AND -B BLOCKING AGENTS FOR PSORIASIS PHOTOTHERAPY
By	Miss Sruangsuda Mawaha
Field of Study	Biotechnology
Thesis Advisor	Assistant Professor Warinthorn Chavasiri, Ph.D.
Thesis Co-Advisor	Nawaporn Vinayavekhin, Ph.D.

Accepted by the Faculty of Science, Chulalongkorn University in Partial Fulfillment of the Requirements for the Master's Degree

.....Dean of the Faculty of Science

(Associate Professor Polkit Sangvanich, Ph.D.)

THESIS COMMITTEE

.....Chairman

(Associate Professor Vudhichai Parasuk, Ph.D.)

.....Thesis Advisor

(Assistant Professor Warinthorn Chavasiri, Ph.D.)

.....Thesis Co-Advisor

(Nawaporn Vinayavekhin, Ph.D.)

.....Examiner

(Associate Professor Aphichart Karnchanatat, Ph.D.)

.....External Examiner

(Assistant Professor Wimonpan Rungprom, Ph.D.)

สรวงสุดา มาเวหา : สารป้องกันรังสียูวี-เอ และยูวี -บี สำหรับการรักษาโรคสะเก็ดเงินด้วยแสง (UV-A AND -B BLOCKING AGENTS FOR PSORIASIS PHOTOTHERAPY) อ.ที่ปรึกษาวิทยานิพนธ์หลัก: ผศ. ดร.วรินทร ชวศิริ, อ.ที่ปรึกษาวิทยานิพนธ์ร่วม: ดร.นวพร วินยเวคิน, 74 หน้า.

สารป้องกันรังสียูวี-เอ และ –บี เป็นองค์ประกอบจำเป็นของครีมทาสำหรับรักษาโรคสะเก็ดเงินด้วยแสง งานวิจัยนี้พบสารผลิตภัณฑ์ธรรมชาติหลายชนิดที่เป็นสารกันรังสียูวี-เอ และ –บี ได้ดี แต่พบจำนวนน้อยที่สามารถดูดกลืนรังสียูวี-บีช่วงแคบ quercetin hydrate, oxyresveratrol และ curcumin เป็นสารกันรังสียูวี-เอ ขณะที่ catechin, hesperetin, lutein และ naringenin เหมาะสำหรับกันรังสียูวี-บี berberine chloride hydrate, berberine และ mansonone G สามารถกันได้ทั้งรังสียูวี-เอ และ –บี เมื่อทดลองสุ่มผสมสารกันรังสี พบว่าของผสมของ mansonone G 0.010 % w/v และ quercetin hydrate 0.0025 % w/v ดีที่สุดสำหรับการพัฒนาเป็นครีมทา ไม่เคยมีรายงานการวิจัยเกี่ยวกับของผสมของสารผลิตภัณฑ์ธรรมชาติ quercetin และ mansonone G ในการนำไปใช้รักษาโรคสะเก็ดเงินด้วยแสง สารผสมดังกล่าวที่ความเข้มข้นต่ำแสดงความเป็นพิษไม่แตกต่างกับสารผสมระหว่าง avobenzone และ octinoxate ที่นิยมใช้ในผลิตภัณฑ์กันแดด สำหรับการทดสอบเสถียรภาพต่อแสง การผสมสารทั้งสองให้ค่าการดูดกลืนแสงที่ความยาวคลื่น 311 นาโนเมตรคงที่ เมื่อสัมผัสแสงแดดไม่เกิน 30 นาที เมื่อเทียบกับสารที่ไม่ได้สัมผัสแสงแดด ในที่สุดได้เตรียมครีมทาสูตรเย็นจากสารทั้งสองชนิดให้เนื้อครีมสีเหลือง

สาขาวิชา เทคโนโลยีชีวภาพ ลายมือชื่อนิสิต .....

ปีการศึกษา 2560 ลายมือชื่อ อ.ที่ปรึกษาหลัก .....

ลายมือชื่อ อ.ที่ปรึกษาร่วม .....

5872117823 : MAJOR BIOTECHNOLOGY
KEYWORDS: PHOTOTHERAPY/ NARROWBAND UV-B/ PSORIASIS/ UV-A/ UV-B

SRUANGSUDA MAWAHA: UV-A AND -B BLOCKING AGENTS FOR PSORIASIS PHOTOTHERAPY. ADVISOR: ASST. PROF. WARINTHORN CHAVASIRI, Ph.D., CO-ADVISOR: NAWAPORN VINAYAVEKHIN, Ph.D., 74 pp.

UV-A and –B blocking agents are essential components for the formulation of topical cream for psoriasis phototherapy. In this research, many natural compounds were discovered as potent UV-A and UV-B blocking agents, but small number could absorb narrowband UV-B. Quercetin hydrate, oxyresveratrol and curcumin were good UV-A blocking agents, while catechin, hesperetin, lutein and naringenin were proper for UV-B blocking agents. Berberine chloride hydrate, demethoxycurcumin and mansonone G were UV-A and –B blocking agents. From random combination, the mixture of mansonone G 0.010 % w/v and quercetin hydrate 0.0025 % w/v was disclosed to be a right choice for this developed topical cream. The combination of truly two natural products as quercetin and mansonone G has never been reported for psoriasis phototherapy. In addition, this combination revealed no difference in cytotoxicity at low concentration from combination of avobenzone and octinoxate (standard compounds). For photostability test, the combination of these two compounds exhibited the same absorption at 311 nm as the unexposed compounds for the period no longer than 30 min. These two compounds were eventually formulated to produce yellow cold topical cream.

Field of Study: Biotechnology
Academic Year: 2017

Student's Signature .....
Advisor's Signature .....
Co-Advisor's Signature .....

ACKNOWLEDGEMENTS

The author wishes to especially be grateful to Assistant Professor Dr. Warinthorn Chavasiri, Natural Product Research Unit (NPRU), Department of Chemistry, Faculty of Science, Chulalongkorn University for his generous guiding, kind help, encouragement and suggestion throughout this research.

Sincere thanks are extended to Associate Professor Dr. Vudhichai Parasuk, Dr. Nawaporn Vinayavekhin, Associate Profrofessor Dr. Aphichart Karnchanatat and Assistant Professor Dr. Wimonpan Rungprom (The Rector of Phranakhon Si Ayutthaya Rajabhat University) serving as the chairman and members of thesis committee, for their valuable comments, discussion and suggestions. Many thanks to Natural Products Research Unit, Department of Chemistry, Faculty of Science, Chulalongkorn University for the support of chemicals and laboratory facilities.

The author would like to thank Ms. Asshaima Paramita Devi, Ms. Suekanya Jaruinthusophon and all members in NPRU and Program in Biotechnology, Faculty of Science, Chulalongkorn University for the advice and scientific techniques during research. Thanks are also extended to my friends and sister for their friendliness, helpful advice, cheerful attitude and encouragement.

Finally, the author wishes to express her deepest appreciation and gratefulness to her parents including Mr. Vera Mawaha and Mrs. Urai Phompagon and my family member for their love, understanding, inspiration, great support and encouragement throughout the entire study.

CONTENTS

Page

Page

Page

LISTS OF TABLES

Page

Page

LISTS OF FIGURES

Page

Page

LIST OF ABBREVIATION

A_t	=	absorbance value of test compound
A_c	=	absorbance value of control
a.u.	=	absorbance unit
ax	=	axial
°C	=	degree Celsius
CO_2	=	carbondioxide
$CDCl_3$-d_1	=	deuterated chlorofrom
d	=	doublet (NMR)
dd	=	doublet of doublet (NMR)
ddd	=	triplet of doublet (NMR)
DCM	=	dichloromethane
DMF	=	*dimethylformamide*
DMSO-d_6	=	dimethyl sulfoxide-d_6
eq	=	equatorial
EtOAc	=	ethyl acetate
EtOH	=	ethanol
g	=	gram
Glc	=	glucose
Rha	=	rhamnose
h	=	hour
Hex	=	hexane
H_2SO_4	=	sulphuric acid
Hz	=	hertz (NMR)
^{1}H NMR	=	proton-1 nuclear magnetic resonance
IC_{50}	=	inbibition concentration at 50 percent

J	=	coupling constant
KOH	=	potassium hydroxide
L	=	liter (s)
M	=	multiplet (NMR)
MeOH	=	methanol
$MgSO_4$	=	magnesium sulfate
min	=	minute
mL	=	milliliter
mM	=	millimolar
NE	=	non effect
nm	=	nanometer
s	=	singlet (NMR)
S.D.	=	standard deviation
t	=	triplet (NMR)
TLC	=	thin layer chromatography
UV	=	ultraviolet
w/v	=	weight by volume
δ	=	chemical shift
µL	=	microliter(s)

CHAPTER I
INTRODUCTION

1.1 Statement and significance of problem

Psoriasis is a disease occurred from genetic disorders and incurable. This disease may be acting up again if the patient was stimulated with many factors such as stress, sun burn and infection *etc*. Nowadays the physician commonly used the sunlight for treatment, so-call "phototherapy". Sunlight consists mostly UV-A (320-400 nm) and UV-B (290-320 nm) that can induce danger to skin. Phototherapy has 3 types: the use of broad-band UV-B, psolalen combined with UV-A (PUVA) and narrow-band UV-B [The wavelength (λ) of 311 nm]. Narrow-band UV-B is effective for many types of skin diseases such as psoriasis and vitiligo *etc*. It is more effective and safer than broad-band UV-B and PUVA, but narrow-band UV-B takes a lot of time and cost. Topical cream containing UV-A and –B blocking agents from natural products is a new choice for phototherapy.

1.2 Psoriasis

Psoriasis is a chronic inflammatory skin disease. It is characterized clinically by sharply demarcated, elevated red scaly plaques (**Figure 1.1**) preferentially occurring at specific body sites, such as elbows, knees and scalp. In severe cases, the whole body may be involved, this serious condition is called erythroderma. Symptoms usually occur first at 20-30 years of age. Twenty to 30% of patients with psoriasis suffer from psoriatic arthritis.

Psoriasis is a multifactorial disease resulting from polygenic predisposition and environmental triggering factors, such as medications, infections or trauma. During the last decades, there is quickly growing understanding of the cellular processes driving inflammation in psoriasis. Importantly, this knowledge might apply for other organ specific autoimmune diseases, such as for Crohn's disease, rheumatoid arthritis and multiple sclerosis, where the affected organs are less accessible than skin [1].

Figure 1.1 Clinical appearance of psoriasis plaques.

1.3 Phototherapy for psoriasis

Goeckerman started using artificial light sources to treat psoriasis patients in the 1920s. The most frequently applied regimen was the combination of crude coal and UV radiation. broad-band UV-B and psoralen plus UV-A therapy (PUVA) has been used since the 1970s [2]. Psoralens, plant-derived photosensitizers, could be applied topically or orally. PUVA therapy had anti-inflammatory and antiproliferative effects, and was highly efficacious for the treatment of psoriasis but has now been mostly discontinued given increased incident of skin cancer because subsequent UV-A irradiation caused a therapeutically beneficial phototoxic reaction to the skin. The effects from UV-A were different from those from UV-B [3].

Furthermore, climatotherapy at the Dead Sea is combined with daily bathing in Dead Sea region that the sunlight can pass only 308 nm. Treatment is usually for four weeks and results in decreases in PASI scores by 75 % or more. Most of the benefit of climatotherapy at the Dead Sea has been attributed to the sunlight at the Dead Sea [4]. In 1980s, narrow-band UV-B was developed and shown to be efficacious. In 1990s, the 308 nm laser was used for the treatment of psoriasis. This laser emitted monochromatic light adjacent to narrow-band UV-B from Dead Sea region, and probably had similar biological and clinical effects [5].

In 1988, Fisher and Parrish used Philips TL-01 fluorescent lamps to deliver narrow-band UV-B for the treatment of psoriasis, following examinations of efficacy of discrete wavelengths in clearing psoriasis [6, 7]. Several studies reported a superior clinical efficacy of narrow-band UV-B to broad-band UV-B [8-11]. Nonetheless, some other studies found that broad-band UV-B and narrow-band UV-B are equally effective [12, 13].

Minimal erythema dose (MED) is the lowest radiation exposure that is sufficient to produce just perceptible erythema on exposed skin after 24 h. Reported MEDs for narrow-band UV-B and broad-band UV-B are shown in **Table 1.1.**

Table 1.1 Minimal erythema dose with narrow-band UV-B and broad-band UV-B**.**

Study	Skin phototype[1]	MED with broad-band UV-B. (mJ/cm^2)	MED with narrow-band UV-B (mJ/cm^2)
Van Weelden [14]	II	76	410
Johnson [2]	II	100	500
Karvonen [15]	II	230	970
Storbeck [16]	II	114	1034
Srinivas [3]	IV	21	300
Tejasvi [4]	III-V	-	1000
Yuon [5]	III-V	-	750-1075
Morita [17]	IV	-	700

Erythema was generated by narrow-band UV-B higher than broad-band UV-B when used narrow-band UV-B was used at 5-times higher than broad-band UV-B [18]. Since in clinical setting, the applied doses are calculated based on the induction of erythema, much higher UV doses are given when narrow-band UV-B is used than in the case of broad-band UV-B. Although in mice narrow-band UV-B was more carcinogenic than broad-band UV-B at equally erythemogen doses [19], follow-up of patients receiving narrow-band UV-B for psoriasis did not show an increase in skin cancer incidence as compared to controls [20-23]. In addition, although narrow-band

UV-B induced the expression of matrix metalloproteinases and reduced the synthesis of collagens by dermal fibroblasts, factors that add to enhanced aging of the skin, these effects were weaker than induced by broad-band UV-B [24].

A further difference between narrow-band UV-B and broad-band UV-B was that narrow-band UV-B radiation did not suppress contact hypersensitivity response in mice, even at 7 times higher doses than the effective broad-band UV-B dose [18], demonstrating that broad-band UV-B and narrow-band UV-B had different biological effects.

In summary, several forms of phototherapy are available for the treatment of psoriasis. Wavelengths between 311-313 nm are probably the most effective in clearing psoriasis. Studies indicated that broad-band UV-B and narrow-band UV-B had different biological effects. Comparing narrow-band UV-B with broad-band UV-B, it was a greater improvement, reduced incidence of burning episodes, increased efficacy and longer remission. For narrow-band UV-B, compared with PUVA it was found that narrow-band UV-B had little overall difference in efficacy but it had lower side effect.

1.4 Mode of action of narrow-band UV-B in psoriasis

Narrow-band UV-B phototherapy reverses keratinocyte proliferation decreases in psoriasis [25, 26]. A number of T lymphocytes in the epidermis and dermis decreases, very suitable due to apoptosis [27, 28] (**Figure 1.2**). The reduction in epidermal T cells correlated with the clinical improvement was not true for the change in dermal T cell numbers [25]. Moreover, decreasing of epidermal T cell numbers also correlated with long-lasting remission after treatment [26]. Surprisingly, recurrent was seen in this study in all patients with remaining keratin 16 staining when finished treatment with narrow-band UV-B .The numbers of epidermal and dermal T cell were more decreased by narrow-band UV-B than broad-band UV-B [27]. It was shown *in vitro* that T lymphocytes were 10-fold more sensitive to the cytotoxic effects of UV-B than keratinocytes, which explained their reduction from the epidermis upon UV-B phototherapy [25]. Moreover, while hyperplastic keratinocytes in untreated psoriasis plaques did not express CD95L/FasL on their plasma membrane, after narrow-band UV-B treatment there was strong and diffuse keratinocyte CD95L/FasL expression that was identical in a temporal

fashion with reduction of intra-epidermal T cells, indicating that a role for FasL in epidermal T cell apoptosis [29].

After 4 weeks of narrow-band UV-B treatment, less IFN-γ and IL-12 and more IL-4 were produced so T cells remained in the lesions [28, 30, 31] (**Figure 1.2**). Only one single dose of broad-band UV-B radiation resulted in decreased IFN-γ production and increased IL-4 production in psoriasis skin, and neutrophils were found to be the source of the increased IL-4 production [32].

The number of Langerhans cells was decreased after narrow-band UV-B phototherapy in non-lesional psoriatic skin [33]. It is not known whether this is the case in the lesion as well.

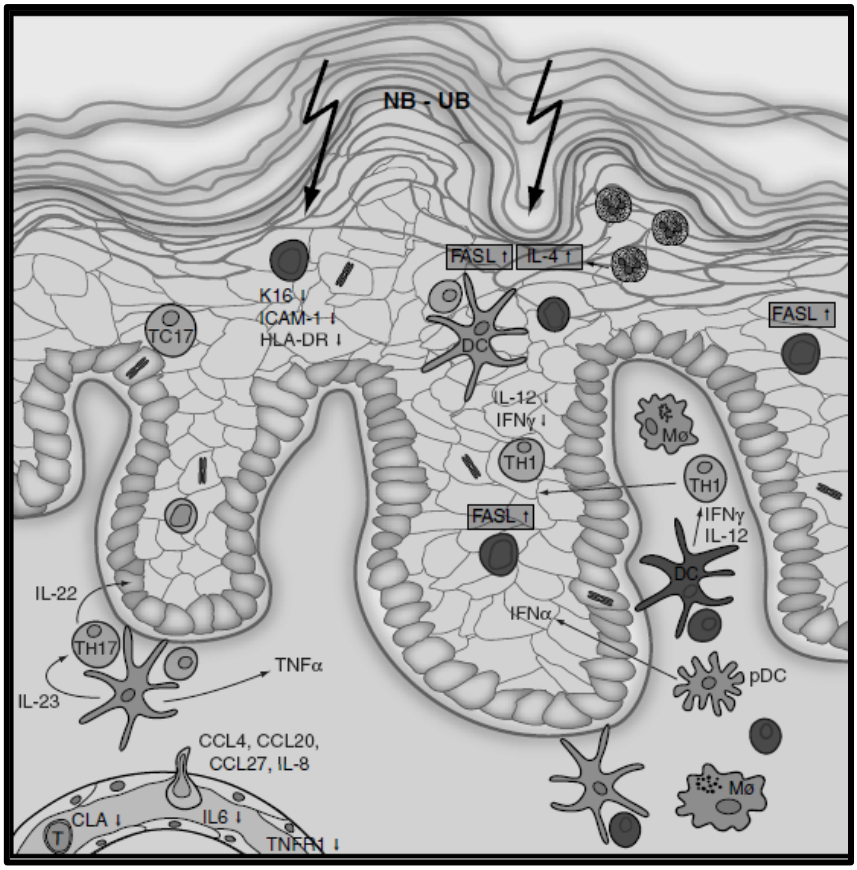

Figure 1.2 Effects of narrow-band UV-B in psoriatic plaques.

1.5 Natural products as UV blocking agents

In 2008, Noratto *et al*. [34] tested the increase of SKU-1064 cells by extracting punicalagins (**Figure 1.3**) as the concentration increased. Punicalagins could inhibit the

growth of skin cells when exposed to UV-A and B-radiation. Punicalagins at concentrations above 2,000 mg/L could reduce reactive oxygen species caused by exposure to UV-A and -B to prevent damage to human skin cells.

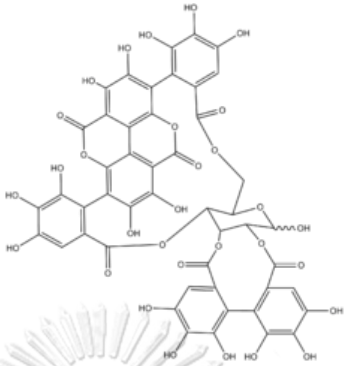

Figure 1.3 Punicalagins.

In 2010s, Jivaramonaikul *et al*. [35] synthesized EH-67 (**Figure 1.4**), a derivative of coumarin extracted from white mustard using Pechmann's reaction. After addition and leaving it for a long time, the UV absorption was unchanged.

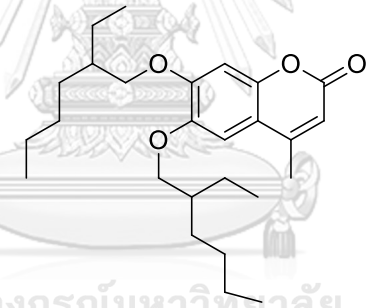

Figure 1.4 EH-67.

In 2011, Korc and Khambholja [36] found that several important substances could be used to protect human skin as a component in sunscreen from UV such as quercetin hydrate (**Figure 1.5**) from onions or tea. In addition, apigenin **(Figure 1.6**) found in *citrus* plants could be used against UV-A and B that may be induced skin cancer. Quercetin hydrate and apigenin had the ability to inhibit the reactive oxygen species, which caused inflammation of the skin and reduce the effect of COL1A1 that was an enzyme building collagen to the skin.

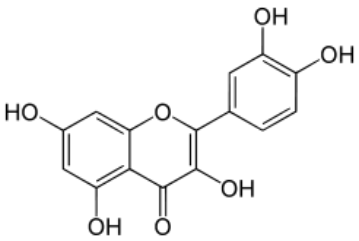

Figure 1.5 Quercetin .

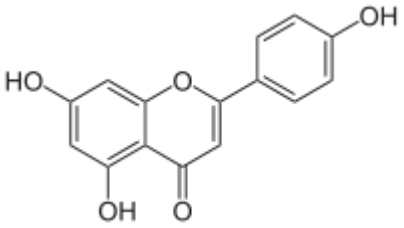

Figure 1.6 Apigenin.

In 2012, Manasathien *et al*. [37] found that the EtOH extracts of pomegranate at 8 mg/mL on mice skin before emitted light 3xMED of UV-B-3 (minimal erythema dose 0.07-0.08 J/mL) for 24 h a week, twice a week for 3 months. This extract could reduce the erythema of the skin by 2.5 times and thickness of skin 1.7 times. Moreover, it lowered sunburn cell by 7.4 times compared with the control and prevented DNA damage of skin cells when exposure with UV-B. In addition, the pomegranate extracts could also protect cells against UV-B.

In 2013, Kantivan [38] addressed that aloe vera gel prevented both UV-A and -B radiation increased moisture and prevented sunburn on the skin. In addition, pomegranate extracts were used because it contained polyphenols (ellagitannins and anthocyanins). The extracts of cucumbers, tomatoes and green tea could also be used because they reduced reactive oxygen species and prevented UV radiation.

In 2014, McCoy *et al*. [39, 40] found that α-glucosyl hesperidin (α-GH, **Figure 1.7**) and diethylamino hydroxybenzoyl hexyl benzoate (DHHB, **Figure 1.8**) were protected against UV-A and -B radiation and did not absorb at 308-311 nm. Narrow-band UV-B was delivered to the skin for treatment of psoriasis and vitillgo. Treatment of a combination of α-GH and DHHB in the topical cream comparing with the Dead Sea region (where can deliver narrow-band UV-B into the ground) revealed that the developed method was more effective than the treatment in the Dead Sea. In addition, the rate of lesion clearance of patients when treated with the topical cream and placebo exhibited more than 50 % and less than 20 %, respectively.

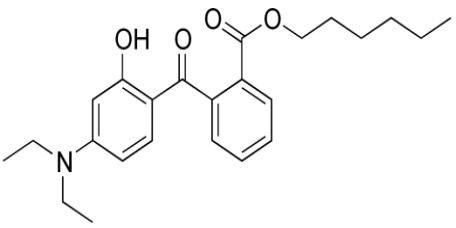

Figure 1.7 DHHB

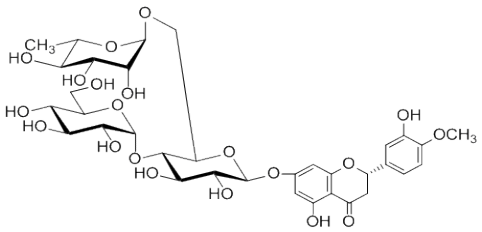

Figure 1.8 α-glycosyl hesperidin

In 2016s, Rojas *et al*. [41] addressed that several compounds could protect against UV-A and -B radiation. The cellular chromophore for UV-A radiation is *trans*-urocanic acid [42], whereas the set of chromophores for UV-B radiations are represented by a wider group composed by nucleic acids, amino acids, (*i.e.*, tryptophan and tyrosine), quinines, flavins, porphyrins, and urocanic acid [43]. There are several processes to control the penetration of UV rays into the skin. The most important are: (i) reflects and occurs at the level of the cornified layer; (ii) diffusion occurs on the cornified layer, especially for melanin that mainly diffuses short wavelengths. Further, (iii) absorption occurs in the cornified layer where 70 % of UV-B is absorbed by the polar amino acids of keratin and urocanic acid, whereas melanin and carotenoids absorb UV rays and visible light, respectively [38]. Other UV protective secondary metabolites were squalane, which was the most important protective lipid of the skin. On the other hand, allantoin is a nucleotide that could absorb UV radiation. Allantoin also healed minor wounds and promoted skin healing [44].

In the last 10 years, a new trend towards naturally occurring compounds has emerged. The production of secondary metabolites in plants is often due to a specific response to their environmental conditions. Thus, several species, especially those exposed to intense radiation have evolved a variety of photoadaptive mechanisms including production of antioxidant and UV absorbing compounds [36].

The light-capturing property of these compounds is correlated to their antiradical activity and is restricted to chemical features such as aromatic rings, cyclic or conjugated double bonds, stereochemistry and typology of substituents [44].

Most of antioxidants are polyphenols that quenched the excited state of the harmful ROS and controlled the multiple signaling pathways neutralizing targets involving in solar damage preventing photo-immunosuppression [45].

Polyphenols are ubiquitous compounds found in most fruits and vegetables and are associated with a wide number of pharmacological activities including antiallergic, antimicrobial, antiviral, anti-inflammatory, hepatoprotective, vasoactive, antithrombotic, antiulcerogenic, antioxidant, free radical scavenging, antitumor, and antiprotozoal properties [46]. They act as reducing agents, hydrogen donors, single oxygen quenchers and potential metal chelators. The beneficial effects of polyphenols, are mainly attributed to their antioxidant or radical scavenging properties. The regular consumption of plants rich in polyphenols is associated with the reduced risk of acquiring cancer, cardiovascular diseases, atherosclerosis, diabetes and Alzheimer's disease [47]. Polyphenols also reduce the scavenging capacity of oxygen free radicals, reduce platelet aggregation and decrease arterial blood pressure. Radical reactions occur in many biological processes as a consequence of living in an oxidizing environment. Differences in the phenolic content of the same extract depend on the extraction procedure, solvent type source and stability in respect to UV radiation. The antimicrobial activity of some polyphenols is explained by the reaction of the bacterial cell with sulfhydryl groups of proteins causing protein precipitation and enzyme inhibition of microorganisms [48, 49].

The number of natural polyphenols has been estimated to be more than 5,000 compounds including 2,000 flavonoids, and new molecules are yet to be discovered. Phenolic compounds as UV blockers could be divided into phenolic acids, terpenoids, monoterpenes, tannins, flavonoids, and volatile oils. Tannins include condensed polymers of catechin or epicatechin and hydrolyzable polymers of gallic or ellagic acids. On the other hand, phenolic acids include hydroxycinnamic compounds such as caffeic, ferulic, *p*-coumaric and their acidic derivatives (*e.g.*, rosmarinic and chlorogenic acids) [50, 51].

Soluble and insoluble polyphenols absorb radiation efficiently in the range of 304-350 and 352-385 nm, respectively. Although these compounds absorb UV light,

they transmit visible and photosynthesis radiation into the mesophyll cells of plants [52].

Phenolic compounds are always present in the form of glycosides in plants and are barely present in free form. Hence, several hydrolytic procedures like acid and alkaline hydrolyses have been used to convert glycosides to aglycones. Moreover, the antioxidant activity of phenolic glycosides is mainly due to the catechol structure in aglycones [53].

Other examples of phenolic compounds comprise kinetin, pycnogenol, allantoin, hesperidin, diosmin, mangiferin, lycopene, and extracts from aloe, horse chestnut, chamomile, comfrey, soy, pomegranate, garlic, and ginger [50-54].

Flavonoids

Flavonoids are non-nutrient secondary metabolites ubiquitous in plants, fruits, and vegetables serving multiple functions including protection from mutagenic UV rays, pollination, feeding deterrence and microbe defense. In humans, they are associated with protection against various diseases, such as cardiovascular and cancer diseases due to their antimutagenic, antimicrobial, antiviral, antiplatelet, antiallergic, estrogenic, antioxidant, anti-inflammatory and sunscreen properties promoting the repair of DNA adducts. The beneficial properties of flavonoids are mostly attributed to their ability to scavenge free radicals, chelate metal ions, activate antioxidant enzymes or inhibit certain enzymatic systems. The antioxidant properties of flavonoids are due to the presence of phenolic groups. Dietary flavonoids are normally found as conjugated glycosides except for fermented foods [55, 56].

Many flavonoids are found to be better antioxidants than ascorbic acid, α-tocopherol, and β-carotene [42]. They are classified as: (i) phenolic, such as catechin; (ii) flavonol, such as quercetin; (iii) flavone, such as diosmetin, and (iv) anthocyanidin [57]. In general, flavonoids show two UV absorption bands, one between 240-280 nm and the other one at 300-370 nm relative to simple phenolics [58, 59]. For instance, quercetin, kaempferol, and isorhamnetin are flavonoids that show UV absorption maxima in the vicinities of 250-280 and 310-385 nm [60]. Quercetin, cyanidin and kaempferol are found in *Hibiscus rosa-sinensis* and *Rosa damascene* flowers. These

compounds are also attributed refrigerant, emollient, demulcent, aphrodisiac, and emmenagogue properties [61].

On the other hand, flavanols from cocoa protected against UV radiation and increased microcirculation in human skin [62]. Daidzin and genistin were found in soybean; puerarin in kudzu, whereas formononetin and biochanin A were found in red clover and chickpea. Conversely, isoflavones were commonly found in passion fruit [63].

Quercetin is a flavonoid of widespread occurrence in nature. It is able to scavenge free radicals generated in aqueous phase, increasing the resistance of lipids against peroxidation. Quercetin exhibited two UV absorption bands at 257 and 373 nm, which were attributed to conjugations in the B and A-rings, respectively [55]. However, it has been proved that the glycosylation of quercetin in rutin decreased its antioxidant and antimicrobial activities [64].

Trans-resveratrol was an antioxidant stilbenoid used in medical applications for lowering the risk of coronary heart disease and had anticarcinogenic properties. It ameliorated the damage caused by UV-B exposure to SKH-1 mice. The protective effects of resveratrol were mediated through its antioxidant potential and its ability to modulate cell cycle and apoptosis signaling pathways. Resveratrol could be found in grape skin, peanuts, soy, tea and other plants. In the human diet, it was regularly introduced mainly through the ingestion of wine, in which both *trans*- and *cis*- isomers were found [65].

Chrysin was a flavonoid found in honey and propolis which inhibited metastasis of cancer cells. Chrysin also displayed antioxidant, anti-inflammatory and antimicrobial activities [66].

Another flavonolignan was silymarin from the fruits and seeds of milk thistle (*Silybum marianum* L.) which has been used to treat liver diseases. Silymarin is a mixture of mainly three flavonolignans: silybin (silybinin), silydianin and silychristin. Silybinin was the major (70-80 %) and most active biological component [51]. Silymarin was a free radical scavenger and inhibited lipid peroxidation and had membrane

stabilizing effects. The UV absorption maximum of silymarin occurred at 287 nm [67-69].

Hesperidin was found in citrus species and was the active constituent of tangerine peel. It had an anti-inflammatory effect by the inhibition of eicosanoids synthesis and had a blood cholesterol lowering effect. It also revealed antimicrobial, antioxidant and diuretic activities. It prevented poisoning caused by heavy metals and also used against diabetes and gastroesophageal reflux diseases. Hesperidin was converted to hesperetin by intestinal microflora and subsequently, absorbed from intestinal mucosa.

Diosmin was a synthetic or modified hesperidin. It was an oral phlebotropic drug used in the treatment of venous and hemorrhoidal diseases. It has anti-inflammatory and antiapoptotic activities and also improves lymphatic drainage by increasing the frequency and intensity of lymphatic contraction and increases the total number of functional lymphatic capillaries [70]. The UV spectra of hesperidin and diosmin in 0.2N NaOH shows a peak at 268 and 285 nm, respectively. Chalcones such as sakuranetin are lipophilic compounds found in trees belonging to *Prunus spp*. (bark and wood), *Eucalyptus spp*. and *Juglans spp*. (bark). It shows the typical peak of flavanone at 280 nm. The addition of NaOAc, $AlCl_3$ or NaOH causes a bathochromic shift to 368 nm [71].

Naringin and rutin are among the most studied flavonoid glycosides. Naringin is a natural flavanone isolated mainly from citric fruit peels such as *Citrus paradisi* and *Citrus aurantium* peel. Naringin has anti-inflammatory, antioxidant, antimicrobial, antiviral, antiulcer, anticarcinogenic and hypolipidemic activities. Naringin may also protect vascular smooth muscle cells by increasing the strength and resistance of blood vessels, and thus has anti-atherogenic effects.

Phytoestrogens

Phytoestrogens are products having estrogenic effects. Soy isoflavones are the most frequently used phytoestrogens and has the potential to reduce the symptoms associated to menopause. Additionally, they prevent chronic pathologies such as osteoporosis, cardiovascular diseases, and hormone-related cancers. Daidzein,

genistein and glycitein are major isoflavones found in soy extracts. They also, occur naturally in soy as their glycosides, named daidzin, genistin and glycitin. When orally administered, isoflavones glycosides undergo enzymatic hydrolysis in the small intestine releasing aglycones which are responsible for their biological effects.

Genistein is the most active compound exhibiting the highest affinity for estrogenic receptors, being approximately ten times more active *in-vivo* than daidzein. After forming a complex with $AlCl_3$, it shows an UV maximum at 382 nm [72].

Carotenoids and xanthophylls

Carotenoids are tetraterpenes and hence contain 40 C-atoms in eight isoprene residues. They all have a center of symmetry. Carotenoids can be further classified into carotenes (pure carbohydrates without additional groups) and xanthophylls (carotenoids containing oxygen). Members of both groups are components of chloroplasts involved in light absorption and photon canalization of photosynthesis [70].

Carotenoids act as antioxidants due to the ability to quench ROS such as singlet molecular oxygen or superoxide, peroxide and hydroxyl radicals generated by exposure to UV radiation. These radicals damage cells by initiating a lipid peroxidation [73]. Carotenoids may be responsible for the decreased cancer incidence associated with the consumption of certain fruits and vegetables. Carotenoids such as alpha-carotene, β-carotene, β-cryptoxanthin and lycopene also contribute to UV protection.

Xanthophyll pigments are derived from carotenoids and also have photoprotective properties. For instance, lutein is derived from carotenes, violaxanthin is a derivative of α-carotene, and zeaxanthin is β-carotene derivative. The supplementation of a combination of β-carotene, lutein, and lycopene at a dose of 8 mg/day is sufficient to ameliorate the UV-induced erythema in humans [74].

The red color of ripe pepper is caused by the presence of lycopene. Likewise, carotenoids precursors such as phytoene and phytofluene are found in tomatoes. Phytoene and phytofluene contribute up to 30% of total carotenoids in tomato [78]. After absorption in the intestine, carotenoids are transported through the bloodstream by lipoproteins to various target tissues. Since carotenoids are lipophilic, they

accumulate in body sites high in total fat levels including the stratum corneum of human skin, the sole of the feet, forehead, the palm of the hands, and adipose tissue [75].

Some of these compounds have a specific function. For instance, zeaxanthin and lutein (isomeric dihydroxy carotenoid) are the major constituents of the retinal macular region and are essential for the visual functionality. The radical scavenging and photoprotective activities are determined by the number of conjugated double bonds and the presence of ionone rings. For instance, lycopene, β-carotene, and zeaxanthin, have a similar hydroxyl radical scavenging ability and contain 11 conjugated double bonds. Conversely, lutein containing only 10 conjugated double bonds, scavenges hydroxyl radicals less effectively. The mechanism of hydroxyl radical scavenging occurs *via* bond formation between the hydroxyl radical and the double bonds in the carotenoid [76].

Catechins

Catechins found in green tea (*Camelia sinensis*) have antifungal activity against *C. albicans*. The major component (epigallocatechin-3-gallate, EGCG) is responsible for its antifungal effects. EGCG and epicatechin-3-gallate are potent inhibitors of the dihydrofolate reductase (DHFR) activity, which is important for cell proliferation and cell growth [77].

Among all the naturally occurring catechins and (-)-epicatechins, when oligomerized exhibit an improved antiproliferative activity. The oligomerization leads to the appearance of a dark-red solution having a new broad absorption peak at 390 nm. These oligomers are water-soluble and stable for three months.

Anthocyanins and proanthocyanidins

Anthocyanins are derived from anthocyanidins by adding sugar [78]. Anthocyanins such as flavonoid glycosides, capensinidin, delphinidin, cyanidin, malvidin, pelargonidin, puchellidin, peonidin, petunidin, rosinidin and tricetinidin have photoprotective properties. They are used in the treatment of circulatory and eye disorders, have free radical scavenging properties and possess radioprotective, anti-inflammatory, anticancer and cardioprotective properties [79]. Proanthocyanidins show

a catechin-like peak at 280 nm [80]. They also have antioxidant activity. For instance, proanthocyanidins from cranberry scavenge ROS and lower the risk of urinary tract infection. In addition, proanthocyanidins have a strong inhibitory capability on pancreatic α-amylase, and thus can be used in the treatment for type II diabetes mellitus.

Polymeric and oligomeric proanthocyanidins, called condensed tannins consist of chains of flavan-3-ol units, (+)-catechin, and (-)-epicatechin linked through C4-C6 and C4-C8 inter flavan bonds. Two popular sources of oligomeric proanthocyanidins are grape seed and pine bark extracts. Cyanidin-3-O-glucoside and cyanidin-3-O-rutinoside are found in red copihue petals [76]. Pelarnidin-3-glucoside is the major anthocyanin component in strawberry (77-95%). Proanthocyanidins are also found in Longan pericarps and in *Pinus radiata* bark [77].

Blueberries (*Vaccinium myrtillus*) have anthocyanins such as cyanidin, delphinidin, malvidin, petunidin, and peonidin which are used to treat a coronary heart disease and urinary tract disord

ers. They also improve visual acuity. The total anthocyanin amount ranges from 300 to 700 mg/100 g [80].

Phenolic acids

This group of polyphenols includes caffeic, ferulic, *p*-coumaric, protocathechuic, *p*-hydroxybenzoic, vanillic and chlorogenic acids, both in free and bonded forms. Most of them are found in *Silphium perfoliatum L*. [49]. The most important phenolic acid is caffeic acid, which is one of hydroxycinnamate and phenylpropanoid metabolites. It is widely distributed in blueberries, coffee drinks, cider and apples. It possesses antioxidant, antiviral, choleretic, cholekinetic, antibacterial and antineoplastic activity *in-vitro*. It combats skin infections such as acne and rosacea. Caffeic acid also shows the angiogenic activity of mononucleus blood leukocytes in healthy humans [81].

Caffeic acid can also be found in ester form with sugar as glycoside bonded with 3,4-dihydroxyphenylethyl alcohol as occur in phenylpropanoids (*i.e.*, echinacosides) found in *Echinacea* genus. On the other hand, ferulic and *p*-coumaric

acids are found in corn, oat and wheat grains. Ferulic acid exhibits a maximum absorbance at 215 nm with additional peaks at 287 and 312 nm. In contrast, *p*-coumaric acid displays a maximum absorbance at 286 nm with additional peaks at 209 and 220 nm [82]. In some cases, the antioxidant activity increases with the number of hydroxyl and methoxy groups. For instance, the catechol group has the ability to enhance the radical scavenging activity due to the *o*-quinone formation. On the other hand, the antioxidant activity does not change in case of esterification of caffeic acid by quinine acid leading to the formation of chlorogenic acid [83].

Triterpenes

Triterpenes are a group of molecules containing 30 C-atoms and are generated by the polymerization of six isoprene units forming pentacyclic triterpenes. Lupeol is a pentacyclic triterpene used to treat cardiovascular ailments, renal disorders, hepatic toxicity, arthritis, diabetes, microbial infections and cancer. Lupeol is also anti-inflammatory, antiangiogenic, antihypercholesterolemic and antioxidative. Lupeol is not toxic in animals at doses ranging from 30 to 2000 mg/kg [84].

Coumarin derivatives

Coumarin is a compound with vanilla-like flavor mainly found in Tonka beans. It is also found in several plants such as lavender, licorice, strawberries, apricots, cherries, cinnamon and sweet clover. Coumarin can occur either free, or combined with glucose (coumarin glycoside). Natural coumarin derivatives such as esculetin, fraxetin, and daphnetin are inhibitors of lipooxygenase and cyclo-oxygenase enzymatic, and neutrophil-dependent superoxide anion systems. For this reason, these coumarins possess anti-inflammatory, anticoagulant, and antioxidant activities [85]

1.6 Cytotoxicity in HaCaT cell [86]

Sunscreen skin penetration and safety could be considered together in order to ensure that in vitro cytotoxicity in human viable epidermis to put the local keratinocyte cell populations at risk of toxicity. The penetration of sunscreen agents in human skin was evaluated after application in mineral oil to isolated human epidermal membranes.

1.7 Objectives of this research

1.7.1 Searching for UV-A & -B blocking agents from natural products.

1.7.2 Developing topical cream for selectively delivering narrow-band UV-B therapy when exposed to sunlight for psoriasis phototherapy.

CHAPTER II

MATERIAL AND METHODS

2.1 Chemicals

The reagents used for synthesis were purchased from Merck chemical company or otherwise stated. All solvents used in this research were purified prior to use by standard methodology except for these which were reagent grades.

2.2 Instruments and equipments

Thin layer chromatography (TLC) was performed on an aluminum sheets precoated with silica gel, Kieselgel 60 F254 (Merck, Germany), column chromatography was performed on silica gel no. 7734 (Merck, Germany). The ^{1}H and ^{13}C spectra were recorded in chloroform-d1 ($CDCl_3$) and dimethyl sulfoxide-*d6* (DMSO-*d6*) on a Varian model Mercury + 400 and a Bruker Advance 400 NMR spectrometer (^{1}H 400 MHz; ^{13}C 100 MHz). UV absorbance measurements were conducted on a 8453 UV/Visible spectrophotometer which was performed by Agilent using standard quartz cells at room temperature and using spectrum mode. The SPF290 was performed by Optometrics Corporation.

2.3 Screening for natural products as UV blocking agents

2.3.1 Natural products from commercial.

Baicalin **(1),** Berberine chloride hydrate **(2)**, Naringenin **(3)**, Quercetin hydrate **(4)** were purchased from TCI. Chrysin **(5)** and catechin **(6)** was purchased from Sigma & Aldrich.

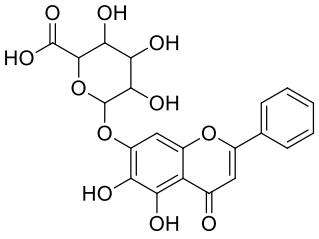

1

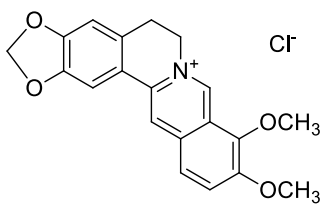

2

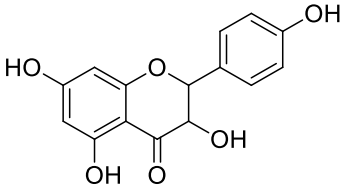

3

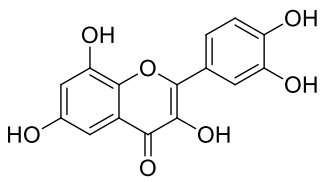

4

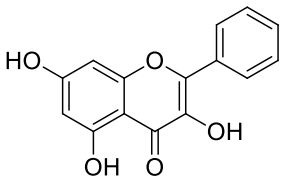

5

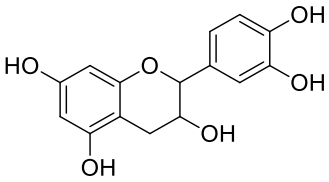

6

2.3.2 Natural products of WC laboratory of chemistry, Chulalongkorn University.

2.3.2.1 6,8 dibromochrysin (7) [87]

6,8 dibromochrysin was synthesized from flavone derivatives by bromination of chrysin. Structure of 6,8 dibromochrysin **(7)** consists of H (R_1), OH (R_2), Br (R_3), OH (R_4), Br (R_5), H ($R_{1'}$), H ($R_{2'}$), H ($R_{3'}$), H ($R_{4'}$) and H ($R_{5'}$). It was obtained as yellow solid.

2.3.2.2 7-methoxy-8-(2'-methoxy-3'-hydroxy-3'-methylbutyl) *coumarin*(8) [88]

The extraction of *Murraya paniculata* was isolated with column chromatograpy. Subfraction 32 was purified by preparative HPLC (CH_3CN: H_2O, 30:70) to give 7-methoxy-8-(2'-methoxy-3'-hydroxy-3'-methylbutyl) coumarin **(8)**. It was obtained as white solid.

2.3.2.3 Phebalosin (9) [88]

The extraction of *Murraya paniculata* was isolated with column chromatograpy. Fraction II-8 was portioned by normal phrase silica gel column. The column was eluted with hexane - EtOAc. The separation of fraction II-8 gave phebalosin **(9)**. It was obtained as pale yellow solid.

2.3.2.4 Murrangatin acetate (10) [88]

The extraction of *Murraya paniculata* was isolated with column chromatography. Fraction I-8 was fractionationed by normal phrase silica gel column. The column was eluted with hexane - EtOAc. The separation of fraction I-8 gave murrangatin acetate **(10)**. It was obtained as green solid.

2.3.2.5 Auraptene (11) [88]

The extraction of *Murraya paniculata* was isolated with column chromatograpy. Fraction II-4 was isolated by normal phrase silica gel column. The II-4

gave auraptene **(11)**. It was obtained as or column was packed with silica gel eluting with hexane - EtOAc gradient. The separation of fraction

2.3.2.6 Oxyresveratrol (12) [89]

The heartwood of *A. lakoocha* was extracted with EtOH after subjected to vacuum liquid chromatography on silica gel eluted with hexane: EtOAc: MeOH (4:6:0.5). Crude oxyresveratrol **(12)** obtained from fractions 6-17 was recrystallized from MeOH to give oxyresveratrol **(12)**.

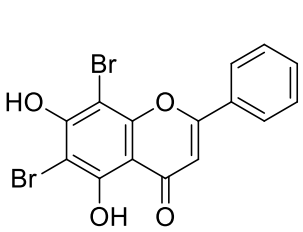

7

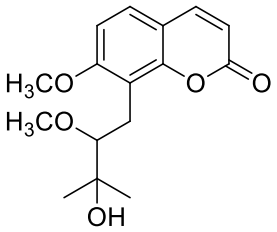

8

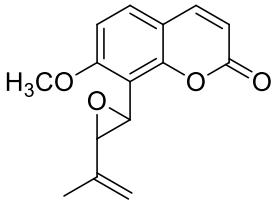

9

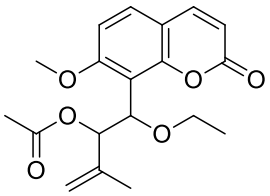

10

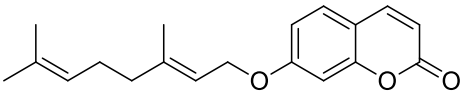

11

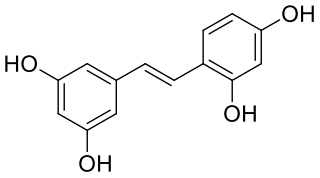

12

2.3.3 Natural products from Extraction, isolation and purification procedure

2.3.3.1 Extraction, isolation of **α**-mangostin (13) [90].

Peel powder of *Garcinia mangostana* Linn. 5.0 g was dissolved in EtOAc. Then the solution was subjected to silica gel quick column eluted with DCM and followed by a mobile phase of 95% DCM in EtOAc to yield 36 Fractions. The isolation of fraction 8-29 gave α-mangostin **(13)**

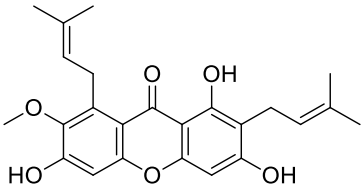

13

α – mangostin **(13)** : yellow solid (71%), R_f 0.62 (solvent system: 95% DCM in EtOAc), ^{1}H NMR (400 MHz, Chloroform-*d*) δ 13.69 (s, 1H), 11.01 (s, 1H), 10.84 (s, 1H), 6.76 (s, 1H), 6.31 (s, 1H), 5.13 (t, *J* = 7.4 Hz, 2H), 3.97 (d, *J* = 7.0 Hz, 2H), 3.67 (s, 3H), 3.17 (d, *J* = 7.3 Hz, 2H), 1.74 (s, 3H), 1.69 (s, 3H), 1.59 (s, 6H).

2.3.3.2 Extraction, isolation of curcumin **(14)**, demethoxycurcumin **(15)** and bis-demethoxycurcumin **(16)**. [91]

Dried powder of *Curcuma longa* 5.0 kg was macerated with EtOAc at room temperature, respectively. The extract was evaporated under vacuum. Then EtOAc extract 50.0 g was subjected to silica gel quick column start with step gradient of 40% EtOAc – 100% EtOAc in hexane to yield 11 fractions. Fraction 2-10 (30 g) was subjected to silica gel column eluted with step gradient of 97% DCM in MeOH– 100% MeOH to give curcumin **(14)**, demethoxycurcumin **(15)** and bis-demethoxycurcumin **(16)**

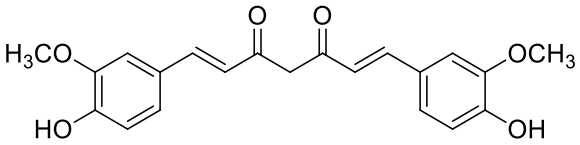

14

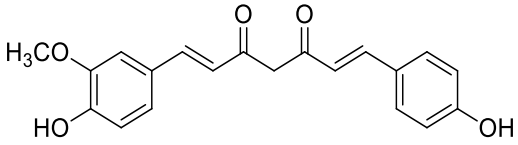

15

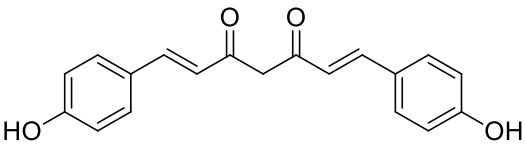

16

Curcumin **(14)**: orange solid (0.50 %), R_f 0.67 (solvent system: 90% DCM in MeOH), ^{1}H NMR (400 MHz, DMSO-d_6) δ 8.70 (s, 1H), 7.54 (d, *J* = 15.8 Hz, 2H), 7.32 (s, 2H), 7.15 (d, *J* = 7.3 Hz, 2H), 6.82 (d, *J* = 7.3 Hz, 2H), 6.75 (d, *J* = 15.8 Hz, 2H), 3.84 (s, 6H), 2.95 – 2.47 (m, 2H).

Demethoxycurcumin **(15)**: orange solid (0.10 %), R_f 0.61 (solvent system: 90% DCM in MeOH), ^{1}H NMR (400 MHz, DMSO-d_6) δ 7.57 (d, *J* = 8.1 Hz, 2H), 7.54 – 7.50

(m, 2H), 7.32 (s, 1H), 7.14 (d, *J* = 8.4 Hz, 1H), 6.81 (d, *J* = 8.1 Hz, 2H), 6.75 (d, *J* = 15.9 Hz, 1H), 6.69 (d, *J* = 15.9 Hz, 1H), 3.83 (s, 3H), 2.84 – 2.20 (m, 2H)

Bis-demethoxycurcumin **(16)**: orange solid (0.04 %), R_f 0.54 (solvent system: 90% DCM in MeOH), ^{1}H NMR (400 MHz, DMSO-d_6) δ 10.05 (s, 1H), 9.15 (s, 1H), 7.57 (d, *J* = 8.6 Hz, 2H), 7.54 (d, *J* = 15.9 Hz, 2H), 6.99 (d, *J* = 15.90 Hz, 2H), 6.82 (d, *J* = 8.3 Hz, 2H), 3.09 – 1.49 (m, 2H)

2.3.3.3 Extraction, purification and conversion hesperidin (17) to hesperetin (18). [92]

Extraction of hesperidin **(17)**:

Air dried sweet orange peels were grinded into powder and Extracted successively amount 12 cycle (total mass of powder is 960 g), 80.0 grams of this powder was placed in a reflux condenser. 600 ml of DCM was added and refluxed for 1.5 h. after filtration of hot mixture through a Buchner funnel, the powder was allowed to dry at room temperature. The dry powder was returned to the flask and 600 mL of methanol was added. The contents were heated under reflux for 2 h again and then hot mixture was filtered. The filtrate was concentrated with distillation column, leaving a syrup residue crystallized from dilute acetic acid (6%), and yielding orange needles (crude hesperidin) melting point was 268°C.

Purification of hesperidin **(17)**:

The crude hesperidin **(17)** was added to DMF (7 mL/ g of syrup) before added acetic acid solution, prepared by warming to about 60 °C a little acetic acid was added. The solution was then filtered through a Buchner funnel, diluted with an equal volume of water and was allowed to stand for 4 h in order to crystallize. The crystals of hesperidin **(17)** were filtered off.

Hydrolysis of Hesperidin into hesperetin :

A mixture of hesperidin **(17)** 9.0 g., MeOH 250 mL. and concentrated H_2SO_4 9 mL was stirred and heated at reflux amount 8 hours. The resulting homogeneous solution was cooled and concentrated and then diluted with EtOAc 500 mL. Every 100 ml of the organic solution is washed with water (4 x 100 mL), and dried with $MgSO_4$. Hesperetin **(18)** was purified by the following procedure: Dissolve the

crude product in minimum of acetone, and the resulting solution was added to a vigorously stirred mixture of H_2O (200 mL) and acetic acid (3mL). In an ice bath, precipitated hesperetin **(18)** was washed and cooled with water. Pure yellow powder of hesperetin **(18)** occurring.

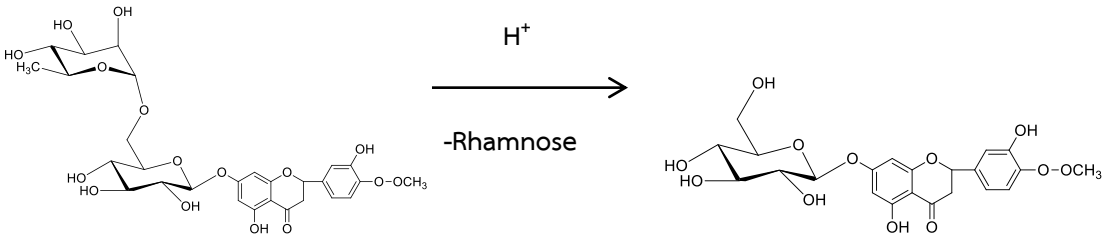

17

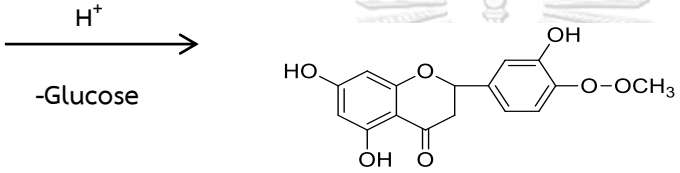

18

Hesperidin **(17)**: yellow solid (10%), R_f = 0.6 (solvent system: butanol /acetic acid/H_2O (4:1:5)), ^{1}H NMR (400 MHz, DMSO-d_6) δ 12.03 (s, 1H), 6.96 (d, J = 8.5 Hz, 1H), 6.91 (d, J = 8.4 Hz, 1H), 6.80 (dd, 1H), 5.50 (dd, J = 11.0, 5.0 Hz, 1H), 4.98 (d, J = 7.0 Hz, 1H), 4.52 (s, 1H), 3.78 (s, 3H), 3.24 (dd, J = 17.0, 3.0 Hz, 1H), 2.78 (dd, J = 17.2, 3.3 Hz, 1H), 1.09 (d, J = 6.0 Hz, 3H).

Hesperetin **(18)**: yellow solid (7.93%), R_f 0.72 (solvent system: 95% MeOH in CH_2Cl_2). ^{1}H NMR (400 MHz, DMSO-d_6) δ 12.05 (s, 1H), 11.02 (s, 1H), 6.92 (dd, *J* = 8.0, 2.0 Hz, 2H), 6.87 (d, *J* = 1.8 Hz, 1H), 6.82 (d, *J* = 2.0 Hz, 1H), 5.88 (d, *J* = 2.7 Hz, 2H), 5.43 (dd, *J* = 11.6, 3.0 Hz, 1H), 3.75 (s, 3H), 3.18 (dd, *J* = 17.2, 12.3 Hz 1H), 2.70 (dd, *J* = 17.2, 3.1 Hz, 1H).

2.3.3.4 Extraction and purification of Lutein **(19)**

Extraction of Lutein **(19)**: [93]

The amount 100.0 g. of dried marigold flower was extracted with 500 mL of hexane in 1 L beaker. The extraction was set up for 4 h in a water bath which was controlled at 40°C. After extraction, the mixture was left to stand for 20 min at room

temperature. The precipitate was isolated and concentrated by a rotary evaporator at 40 °C. The extraction solid was marigold oleoresin which was collected in a refrigerator at -20 °C.

Saponification step:

The amount 0.6 g. of KOH was dissolved in 10 ml of EtOH in a 125 ml flask, into which 1.0 g. of marigold oleoresin was added. The flask was shaken at 150 rpm and 50°C for 4 h. Then, 50 ml of ethanol was added into the flask, and this mixture was then transferred to a separation funnel, into which 100 mL of 5% Na_2SO_4 solution and 80 mL of diethyl ether were added. All components were separated into two phases. The upper phase (ether fraction) was collected as free lutein stock solution. Free lutein stock solution was extracted repeatedly with water until the water phase became colorless.

Purification of Lutein **(19)**: [94]

The dried product from saponification step was dissolved in 50 mL hexane: acetone (4:1) and stirred for 30 min at room temperature. The precipitated xanthophyll crystals were washed with a mixture of hexane 60 mL and cold ethanol 50 mL. The final product, orange crystals of lutein **(19)**, was vacuum dried at 39 ° C.

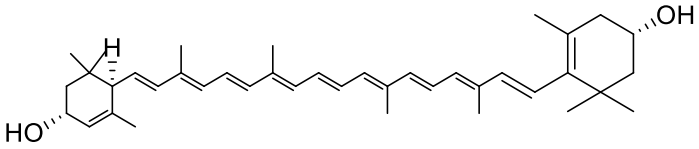

19

Lutein **(19)**: orange solid (9.17%), R_f 0.25 (solvent system: hexane/ EtOAc/ acetone/ MeOH (27:4:2:2)). ^{1}H NMR (400 MHz, DMSO-d_6) δ 7.26 (s, 4H), 5.59 – 5.06 (m, 5H), 4.29 (d, *J* = 13.0 Hz, 1H), 4.18 – 4.08 (m, 1H), 1.58 (s, 18H), 1.29 (s, 12H), 1.07 (d, *J* = 13.0 Hz, 2H), 0.99 (d, *J* = 13.0 Hz, 1H), 0.88 (t, 3H).

2.3.3.5 Mansonone G **(20)** [95]

Dried powder of *Mansonia gagei* Heartwoods 5.0 kg was extracted by soaking in ethyl acetate EtOAc at room temperature, leaving for two days, filtering, and evaporating. This step was repeated four times with fresh solvent. The crude EtOAc extract was obtained as dark-brown. The EtOAc extract of *M. gagei* heartwoods (260 g) was subjected to silica gel column. The column was initially eluted with a mixture of 20% EtOAc in hexane then followed by increasing polarity with a mixture of EtOAc in hexane (25-80%), EtOAc 100%, MeOH in EtOAc (5–10%) and final with MeOH 100%. Approximately 0.5 L of solvent was collected for each fraction and then evaporated the solvent using vacuum rotary evaporator. It gives yield 9 fractions. The fraction 3 and 4 were further separated by using silica gel column. The columns were eluted with step gradient of hexane - EtOAc and EtOAc - MeOH as solvent systems. Mansonone G **(20)** as a major compound of these fraction were obtained.

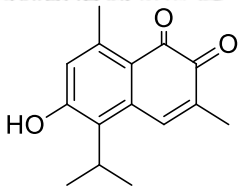

20

Mansonone G **(20)**: red brown solid (0.17%), R_f 0.27 (solvent system: hexane/ EtOAc/ MeOH (6:3:0.05)), ^{1}H NMR (400 MHz, DMSO d_6) δ 7.87 (s, 1H), 6.63 (s, 1H), 4.03 (q, J = 7.0 Hz, 1H), 3.63 (s, 1H), 2.45 (s, 3H), 1.95 (s, 3H), 1.34 (d, J = 7.0 Hz, 6H).

2.3.3.6 Piperine **(21)**[96]

Black pepper powder 5.0 g and 50 mL of DCM was refluxed for 20 min. Suction filter the slurry with Buchner funnel, washing the pepper grounds once with 5 mL of DCM. The extract was concentrate in vacuum evaporator. The resulting showed olive-brown. Then cold ether was added to the extract and stirring for 3-4 min. Some piperine may precipitate at this point, but remove the solvent in vacuum evaporator. Isolate the straw-yellow crystals of crude piperine by suction filtration and wash the crystals twice with 2 mL of cold ether. Recrystallization the crude piperine by dissolve it in a minimum amount of hot 3:2 acetone:hexane solution. Allow the solution to sit undisturbed for 15 min at room temperature. Rod-like,

yellow crystals of piperine **(21)**should be present. Cool the solution for an additional 30 min in an ice-bath before isolating the purified piperine **(21)** by suction filtration Wash the crystals once with a 2 mL portion of cold ether, allow them to air dry for several minutes.

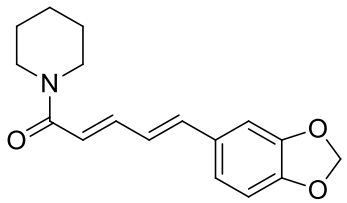

21

Piperine **(21):** yellow crystal solid (0.17%), ^{1}H NMR (400 MHz, Chloroform-*d*) δ 7.45 (ddd, *J* = 14.7, 8.5, 1.8 Hz, 1H), 6.97 (d, *J* = 1.6 Hz, 1H), 6.87 (dd, *J* = 8.0, 1.6 Hz, 1H), 6.82 (d, *J* = 8.0 Hz, 1H), 6.81 (d, *J* = 15.0 Hz, 1H), 6.76 (dd, *J* = 15.0, 8.5 Hz, 1H), 6.45 (d, *J* = 14.7 Hz, 1H), 5.99 (s, 2H), 3.61 (s, 2H), 3.58 (s, 2H), 2.28 (s, 2H), 1.74 – 1.54 (m, 6H).

2.4 UV spectrum measurements.

All of natural products were determined spectrum by using 8453 UV/Visible spectrophotometer. Start with warmed lamp for 45 minutes. And then spectrum was set up as task and selected the range of wavelength from 280 to 400 nm. After that the experiment used 1.0 cm. quartz cuvette for collect sample. All samples were prepared at the concentration 0.010, 0.0050, 0.0025, 0.0010 %w/v in DMF. Absorbance value and spectrum was measure three replicate.

2.5 Cytotoxicity in Human Keratinocyte (HEK) Cultures by MTT assay and photostability.

2.5.1 Cytotoxicity [86]

Toxicity Testing was studied at faculty of pharmaceutical sciences, Chulalongkorn University. HaCaT cell were used as testing. The monolayer cell culture was trypsinized and the cell count was adjusted to 3-lakhcells/ml using medium containing 10% newborn calf serum. To each well of 96 well microlitre plates, 0.1ml of diluted cell suspension was added. After 24 hours, when the monolayer formed the

supernatant was flicked off and 100 µl of different test compounds were added to the cells in microtitre plates and kept for incubation at 37ºC in 5 % CO2 incubator for 24 hour and cells were periodically checked for granularity, shrinkage, swelling. After 24 hour, the sample solution in wells was flicked off and 50 µl of MTT dye was added to each well. The plates were gently shaken and incubated for 3 h. at 37°C in 5% CO_2 incubator. The supernatant was removed, 50 µl of DMSO was added, and the plates were gently shaken to solubilize the formed formazan. The absorbance was measured using a microplate reader at a wavelength of 517 nm. The percentage growth inhibition was calculated using the formula below: The percentage growth inhibition was calculated using following formula,

$$\% \text{ cell viability} = \frac{\text{Absorbance value of test}}{\text{Absorbance value of control}} \times 100$$

2.5.2 Photostability

Each of natural products in combination at the proper concentration were put in one dark bottle 1:1 ratio (5 ml: 5 ml) for standing in dark area 1 h and clearly bottom for exposure with sunlight 5 min, 15 min, 30 min and 1 h and solar stimulator machine 1 h also. Then each of bottle were measured the absorbance with 8453 UV/Visible spectrophotometer as three replicates. The results were presented as spectrum.

2.6 Formulation of the topical cream

The suitable ratio of absorber agents were formulated into Cold cream which was supported by Chulalongkorn Hospital.

CHAPTER III

RESULTS AND DISCUSSION

The main objective of this research is to search for the UV blocking agents from natural resources to use as one of ingredients in the topical cream for psoriasis phototherapy. The ideal UV blocking agents should weakly absorb at 311 nm while intensely absorb UV-A or –B. The concentration of selected natural products was varied to find the optimal value. The best components were randomly combined, tested for toxicity and photostability, and finally selected for the best combination for topical cream.

3.1 Screening for natural products as UV blocking agents

Certain natural products were selected to screen for their ability to serve as UV blocking agents. Typically, plant materials were extracted with a proper solvent to yield the extract which further purified by separation using column chromatography. Nine compounds were finally obtained and characterized for their identities by using spectroscopic evidence.

3.1.1 Separation and purification of α-mangostin **(13)**

The isolation of α-mangostin **(13)** was accomplished by silica gel column of the EtOAc extract of the pericarps of *Garcinia mangostana* Linn. The target product was obtained as orange solid. The ^{1}H NMR spectrum of **13** is presented in Figure 3.1

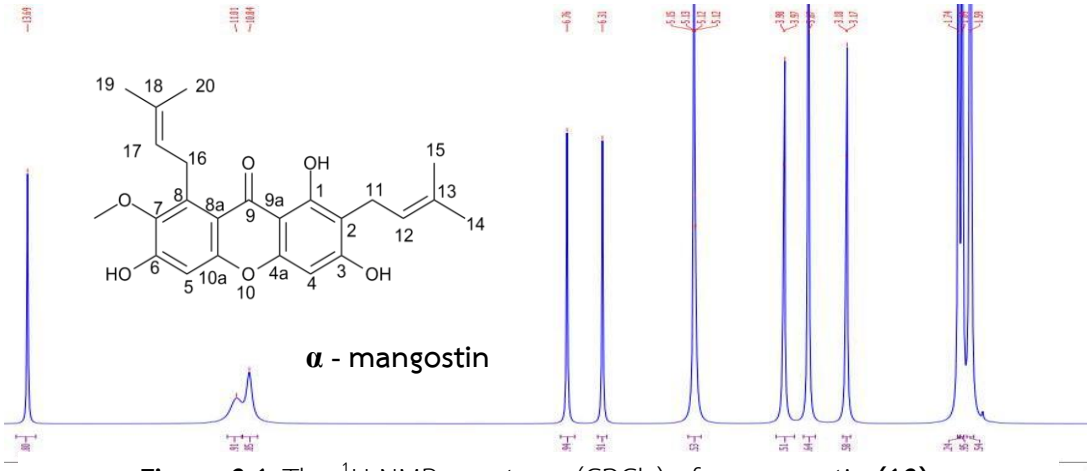

Figure 3.1 The ^{1}H NMR spectrum ($CDCl_3$) of α-mangostin **(13).**

The structural characterization of α-mangostin **(13)** was conducted by comparing spectroscopic data with previous studies [107,108]. The ^{1}H NMR spectral assignment of α-mangostin **(13)** is presented in **Table 3.1**.

Table 3.1 The 1H NMR spectral assignment of α-mangostin **(13).**

Position	Chemical shift (ppm)	
	α-mangostin (DMSO)	**Compound 13**
1-OH	13.72 (s)	13.69 (s)
3-OH	-	11.01 (s)
4	6.28 (s)	6.31 (s)
5	6.80 (s)	6.76 (s)
6-OH	-	10.84 (s)
11	3.35 (d, *J*=7.3 Hz)	3.17 (d, *J* = 7.3 Hz)
12	5.17 (t, *J*=7.3 Hz)	5.13 (t, *J* = 7.4 Hz)
14-Me	1.77 (s)	1.74 (s)
15-Me	1.63 (s)	1.59 (s).
16	4.04 (d, *J*=7.0 Hz)	3.97 (d, *J* = 7.0 Hz)
17	5.17 (t, *J*=7.3 Hz)	5.13 (t, *J* = 7.4 Hz)
19-Me	1.71 (s)	1.59 (s)
20-Me	1.73 (s)	1.69 (s)
7-OMe	3.71 (s)	3.67 (s)

3.1.2 Separation and purification of curcumin **(14)**, demethoxycurcumin **(15)** and bis-demethoxycurcumin **(16)**

The EtOAc extract from dry powder of *Curcuma longa* was subjected to silica gel column eluting with a mixture of 97% DCM in MeOH to furnish curcumin **(14)**, demethoxycurcumin **(15)** and bis-demethoxycurcumin **(16)**. The structural characterization of three compounds was conducted by comparing spectroscopic data with previous report [98]. The comparative NMR spectral assignment of **14-16** is presented in **Figures 3.2-3.4** and **Table 3.2**.

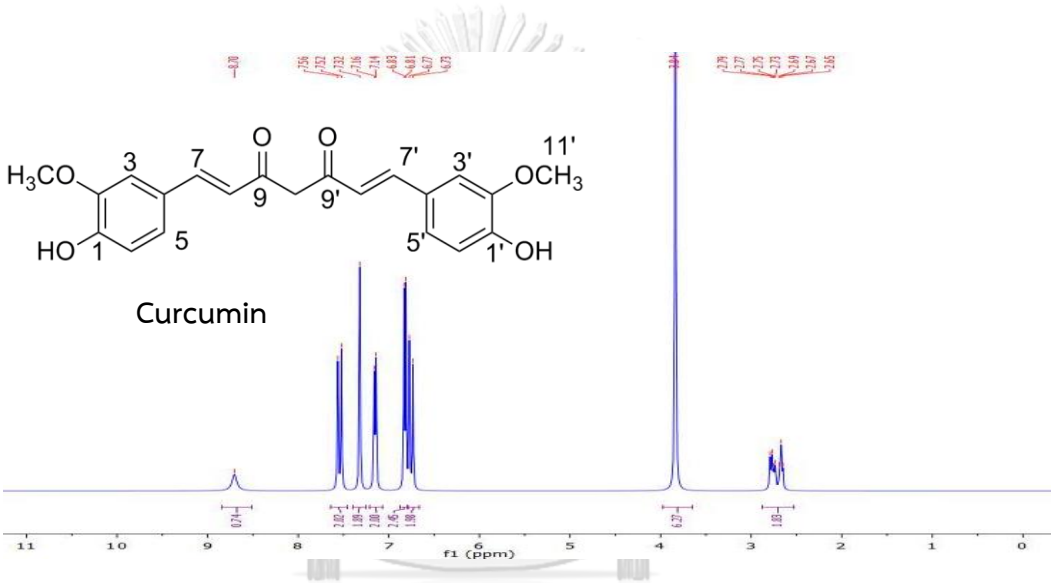

Figure 3.2 The ^{1}H NMR spectrum ($CDCl_3$) of curcumin **(14).**

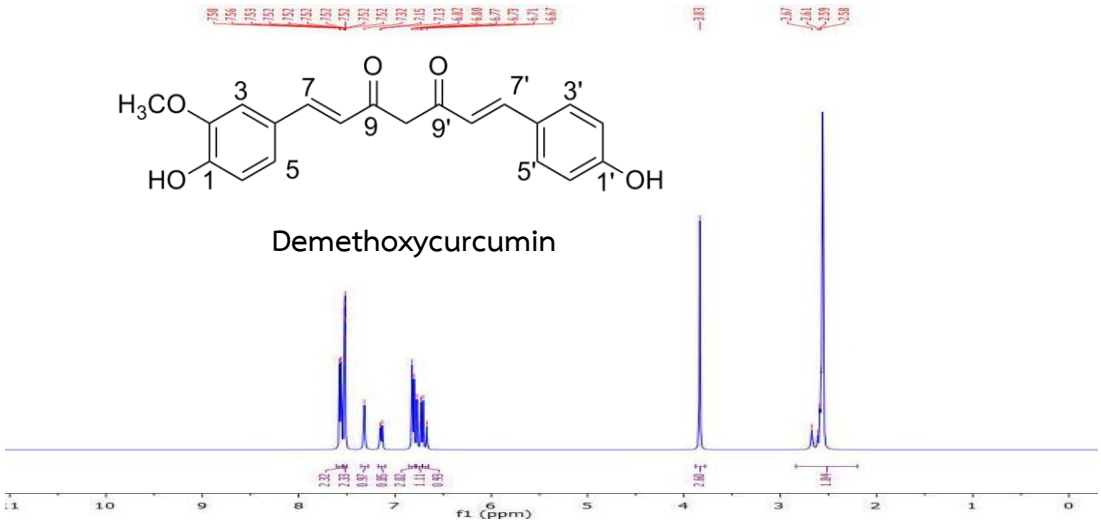

Figure 3.3 The ^{1}H NMR spectrum ($CDCl_3$) of demethoxycurcumin **(15)**.

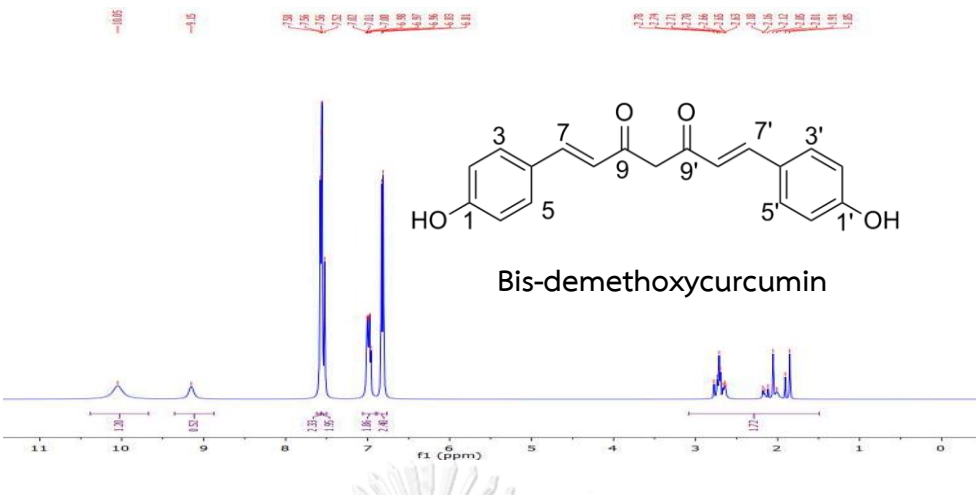

Figure 3.4 The ^{1}H NMR spectrum ($CDCl_3$) of bis-demethoxycurcumin **(16)**.

Table 3.2 The ^{1}H NMR spectral assignment of curcumin (Cur, 14),demethoxycurcumin (DMC, 15) and bisdemethoxycurcumin (BDMC, 16)

Position	Chemical shift (ppm)					
	Cur	Compound 14	DMC.	Compound 15	BDMC.	Compound 16
1-OH	9.70 (s)	-	-	-	-	9.15 (s)
3	7.31 (s)	7.32 (s)	7.32 (s)	7.32 (s)	7.56 (d, *J* = 8.6 Hz)	7.57 (d, *J* = 8.6 Hz)
5	7.15 (d, *J* = 7.3 Hz)	7.15 (d, *J* = 7.3 Hz)	7.15 (d, *J* = 8.3 Hz)	7.14 (d, *J* = 8.4 Hz)	7.56 (d, *J* = 8.6 Hz)	-
6	6.82 (d, *J* = 7.3 Hz)	6.82 (d, *J* = 7.3 Hz)	6.82 (d, *J* = 7.3 Hz)	6.81 (d, *J* = 8.1 Hz)	6.82 (d, *J* = 8.6 Hz)	6.82 (d, *J* = 8.3 Hz)
7	7.54 (d, *J* = 15.7 Hz)	7.54 (d, *J* = 15.8 Hz)	7.54 (m)	7.52 (m)	7.54 (d, *J* = 15.9 Hz)	7.54 (d, *J* = 15.9 Hz)
8	7.75(d, *J* =15.7 Hz)	6.75 (d, *J* = 15.8 Hz)	6.75 (d, *J* = 15.9 Hz)	6.75 (d, *J* = 15.9 Hz)	6.86 (d, *J* = 15.9 Hz)	6.99 (d, *J* = 15.90 Hz)
10	4.13 (m)	2.74 (m)	4.13 (m)	2.58 (m)	4.13 (m)	2.42 (m)
11-OMe	3.83 (s)	3.84 (s)	3.84 (s)	3.83 (s)	-	-
1'-OH	9.70 (s)	8.70 (s)	-	-	10.07 (s)	10.05 (s)
2'	-	-	6.83 (d, *J* = 8.1 Hz)	6.81 (d, *J* = 8.1 Hz)	6.82 (d, *J* = 8.6 Hz)	-
3'	7.31 (s)	7.32 (s)	7.56 (d, *J* = 8.1 Hz)	7.57 (d, *J* = 8.1 Hz)	7.56 (d, *J* = 8.6 Hz)	7.57 (d, *J* = 8.6 Hz)
5'	7.15 (d, *J* = 7.3 Hz)	7.15 (d, *J* = 7.3 Hz)	7.56 (d, *J* = 8.1 Hz)	7.57 (d, *J* = 8.1 Hz)	7.56 (d, *J* = 8.6 Hz)	-
6'	6.82 (d, *J* = 7. 3 Hz)	6.82 (d, *J* = 7.3 Hz)	6.83 (d, *J* = 8.1 Hz)	6.81 (d, *J* = 8.1 Hz)	6.82 (d, *J* = 8.6 Hz)	6.82 (d, *J* = 8.3 Hz)
7'	7.54 (d, *J* = 15.7 Hz)	7.54 (d, *J* = 15.8 Hz)	7.54 (m)	7.52 (m)	7.54 (d, *J* = 15.9 Hz)	7.54 (d, *J* = 15.9 Hz)
8'	7.75 (d, *J* = 15.7 Hz)	6.75 (d, *J* = 15.8 Hz)	6.69 (d, *J* = 15.9 Hz)	6.69 (d, *J* = 15.9 Hz)	6.86 (d, *J* = 15.9 Hz)	6.99 (d, *J* = 15.90 Hz)
11'-OMe	3.83 (s)	3.84 (s)	-	-	-	-

The appearance of methoxy protons at δ_H 3.83 and 3.84 ppm indicated the existence of curcumin **(14)** and demethoxycurcumin **(15)**, while the absence of methoxy protons at δ_H 3.83-3.84 ppm revealed the accomplishment of the isolation of bis-demethoxycurcumin (16).

3.1.3 Separation, purification of hesperidin **(17)** and conversion of hesperidin to hesperetin **(18)**

Orange peel powder was added DCM and refluxed for 1.5 h. The residue was further extracted with MeOH and refluxed for 2 h. Then the MeOH extract was filtered and purified by recrystallization in DMF.

Hesperidin **(17)** was hydrolyzed to convert to hesperetin **(18)**. The structural characterization of hesperidin **(17)** which was hesperetin-7-*O*-rutinoside and hesperetin (acid hydrolysis product of hesperidin, **18**) was shown in **Figures 3.5, 3.6** and **Table 3.3**, and compared with previous study [99

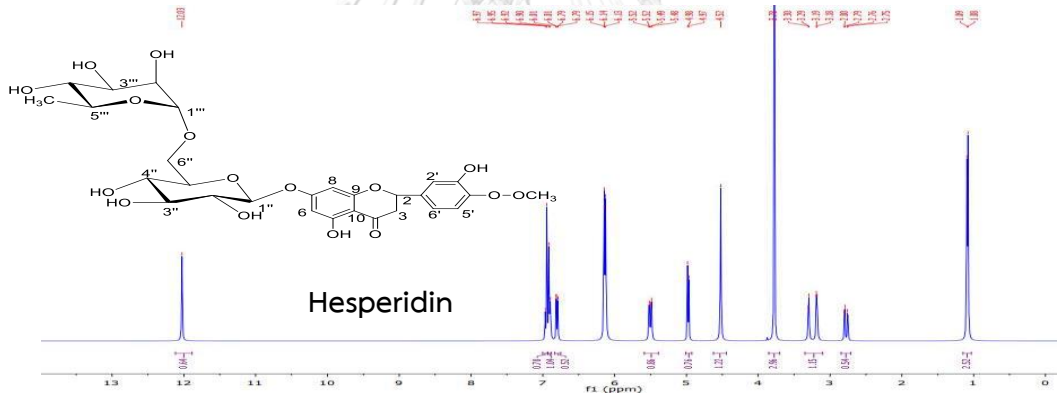

Figure 3.6 The ^{1}H NMR spectrum ($CDCl_3$) of hesperidin **(17)**.

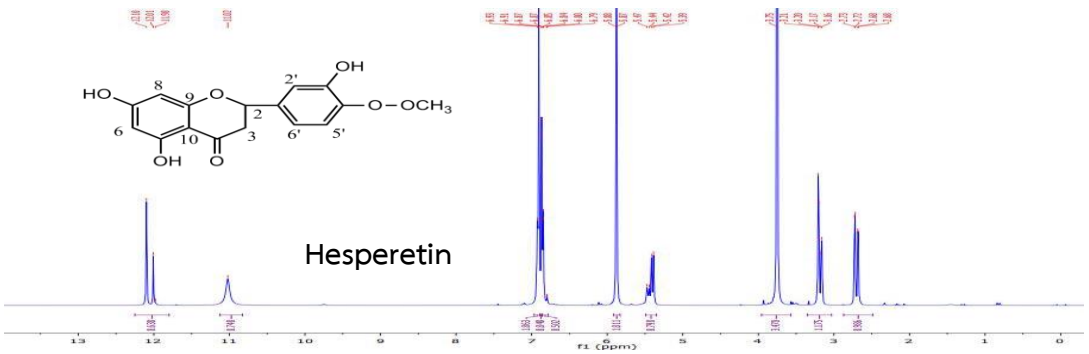

Figure 3.5 The ^{1}H NMR spectrum ($CDCl_3$) of hesperetin **(18).**

Table 3.3 The ^{1}H NMR spectral assignment of hesperidin **(17)** and hesperetin **(18)**.

Position	Chemical shift (ppm)			
	Hesperidin	Compound 17	Hesperetin	Compound 18
2	5.54 (dd, *J* = 7.8, 3.0 Hz)	5.50 (dd, *J* = 11.0, 5.0 Hz)	5.46 (dd, *J* = 12.3, 3.0 Hz)	5.43 (dd, *J* = 11.6, 3.0 Hz)
3-ax	2.79 (dd, *J* = 17.4, 3.0 Hz)	2.78 (dd, *J* = 17.2, 5.0 Hz)	2.74 (dd, *J* = 17.2, 3.0 Hz)	2.70 (dd, *J* = 17.2, 3.1 Hz)
3-eq	3.31 (dd, *J* = 17.3, 8.1 Hz)	3.24 (dd, *J* = 17.4, 3.0 Hz)	3.23 (dd, *J* = 17.2, 12.3 Hz)	3.18 (dd, *J* = 17.2, 12.3)
5	-	12.03 (s)	-	12.05 (s)
6	6.18 (d, *J* = 2.4 Hz)	6.12 (d, *J* = 2.0 Hz)	5.91 (d, *J* = 1.9 Hz)	5.88 (d, *J* = 2.7 Hz)
7	-	-	-	11.02 (s)
8	6.16 (d, *J* = 3 Hz)	6.15 (d, *J* = 2.4 Hz)	5.92 (d, *J* = 1.9 Hz)	5.88 (d, *J* = 2.7 Hz)
2'	6.97 (d, *J* = 1.6 Hz)	6.96 (d, *J* = 2.0 Hz)	6.95 (d, *J* = 1.6 Hz)	6.87 (d, *J* = 1.8 Hz)
5'	6.83 (d, *J* = 8.4 Hz)	6.91 (d, *J* = 8.4 Hz)	6.97 (d, *J* = 8.2 Hz)	6.82 (d, *J* = 2.0 Hz)
6'	6.99 (dd, *J* = 7.9, 1.6 Hz)	6.80 (dd, *J* = 8.0, 2.0 Hz)	6.90 (dd, *J* = 8.2, 1.6 Hz)	6.92 (dd, *J* = 8.0, 2.0 Hz)
4'-OMe	3.81 (s)	3.78 (s)	3.81 (s)	3.75 (s)
Glc-1''	5.01 (d, *J* = 7.7 Hz)	4.98 (d, *J* = 7.0 Hz)	-	-
Rha-1'''	4.55 (d, *J* = 2.9 Hz)	4.52 (s)	-	-
5'''	1.12 (d, *J* = 6.6 Hz)	1.09 (d, *J* = 6.0 Hz).	-	-

3.1.4 Separation and purification of lutein (19)

Lutein **(19)** was a dried saponified product from marigold flower (*Tagetes erecta)* powder. The structural characterization of target compounds was conducted by comparing spectroscopic data with previous study [100]. The NMR spectral data of lutein **(19)** is presented in **Figure 3.7** and **Table 3.4-3.5**, respectively.

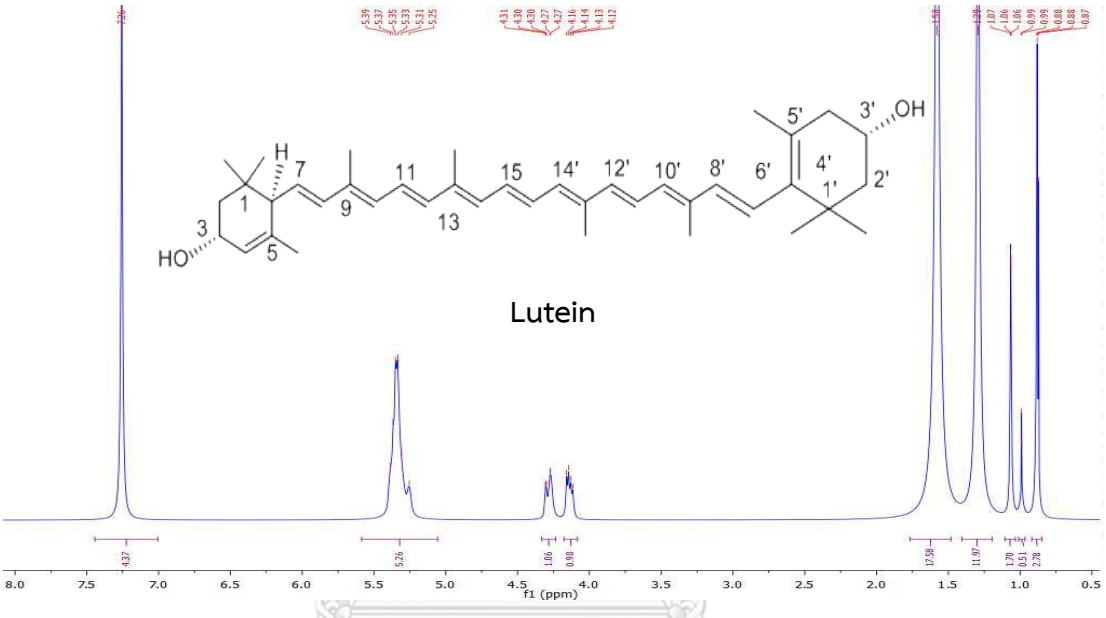

Figure 3.7 The ^{1}H NMR spectrum ($CDCl_3$) of lutein **(19)**.

Table 3.4 The ^{1}H NMR spectral assignment of lutein **(19)**.

Position	Chemical shift (ppm)	
	Lutein	**Compound 19**
1-gem-Me	0.85, 0.99 (s)	1.29 (s), 1.58 (s)
2	1.48 (t)	0.88 (t, *J* = 12.0, 13.0 Hz)
3-OH	4.0 (m)	4.14 (m)
4	1.48 (t, *J* = 12.0 Hz)	0.88 (t, *J* = 12.0 Hz, 13.0 Hz)
5-Me	1.74 (s)	1.29 (s)
6	1.84 (dd, *J* = 13.0 Hz)	1.07 (d, *J* = 13.0 Hz)
7	6.12 (s)	7.26 (s)
8	6.12 (s)	7.26 (s)
9-Me	1.97 (s)	1.58 (s)
10	6.15 (m)	5.36 (m)
11	6.64 (m)	-
12	6.36 (d, J = 15.0 Hz)	-
13-Me	1.97 (s)	1.58 (s)
14	6.26 (m)	5.36 (m)
15	6.63 (m)	-
1'-gem-Me	0.85, 0.99 (s)	1.29 (s), 1.58 (s)
2'	1.84 (dd, J = 13.0 Hz)	1.07 (d, J = 13.0 Hz)
3'-OH	4.25 (m)	4.29 (m)
4'	5.55 (s)	7.26 (s)
5'-Me	1.63 (s)	1.29 (s)
6'	2.04 (dd, J = 17, 10 Hz)	0.99 (d)
7'	5.43 (dd, J = 15.5,10 Hz)	7.26 (s)
8'	6.15 (m)	5.36 (m)
9'-Me	1.91 (s)	1.58 (s)
1'-gem-Me	0.85, 0.99 (s)	1.29 (s), 1.58 (s)
2'	1.84 (dd, J = 13.0 Hz)	1.07 (d, J = 13.0 Hz)
3'-OH	4.25 (m)	4.29 (m)
4'	5.55 (s)	7.26 (s)

Table 3.5 The ^{1}H NMR spectral assignment of lutein (19) continued.

Position	Chemical shift (ppm)	
	Lutein	Compound 19
4’	5.55 (s)	7.26 (s)
5’-Me	1.63 (s)	1.29 (s)
6’	2.04 (dd, *J* = 17, 10 Hz)	0.99 (d)
7’	5.43 (dd, *J* = 15.5,10 Hz)	7.26 (s)
8’	6.15 (m)	5.36 (m)
9’-Me	1.91 (s)	1.58 (s)
10’	6.15 (m)	5.36 (m)
11’	6.64 (m)	-
12’	6.36 (d)	-
13’-Me	1.97 (s)	1.58 (m)
14’	6.26 (m)	5.36 (m)

3.1.5 Separation and purification of mansonone G **(20)**

The separation of the EtOAc extract of *Mansonia gagei* heartwoods led to the isolation of mansonone G **(20)**. The structural identification of this compound was conducted by comparing spectroscopic data with previous study [109]. The ^{1}H NMR spectral data assignment of mansonone G **(20)** is presented in **Table 3.6**.

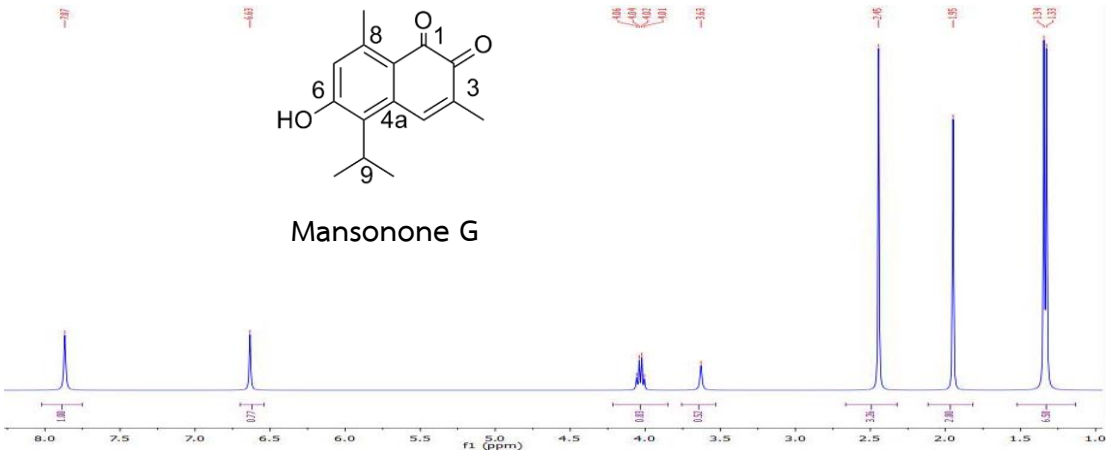

Figure 3.8 The ^{1}H NMR spectrum ($CDCl_3$) of mansonone G **(20)**.

Table 3.6 The ^{1}H NMR spectral assignment of mansonone G **(20)**.

Position	Chemical shift (ppm)	
	Mansonone G (DMSO)	Compound 20
3	7.71 (s)	7.87 (s)
4	6.57 (s)	6.63 (s)
6-OH	1.94 (s)	3.63 (s)
9	3.5 (m)	4.03 (q, *J* = 7.0 Hz)
10-Me	1.25 (d, *J* = 7.0 Hz)	1.34 (d, *J* = 7.0 Hz)
11-Me	1.25 (d, *J* = 7.0 Hz)	1.34 (d, *J* = 7.0 Hz)
12-Me	2.56 (s)	2.45 (s)
13-Me	1.29 (d, *J* = 7.0 Hz)	1.95 (s)

3.1.6 Separation and purification of piperine **(21)**

The separation of the DCM extract of black pepper fruit (*Piper nigrum*) powder yielded piperine **(21)**. The chemical shifts of the target molecule are tabulated in **Table 3.7** and compared spectroscopic data with previous study [110]. The spectrum is shown in **Figure 3.9**.

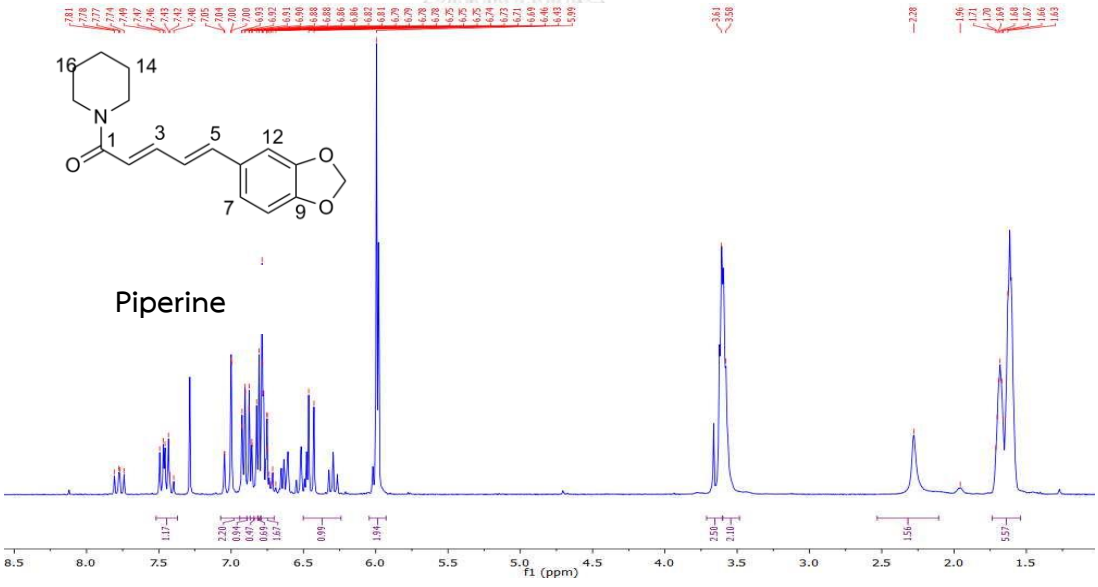

Figure 3.9 The ^{1}H NMR spectrum ($CDCl_3$) of piperine **(21)**.

Table 3.7 The ^{1}H NMR spectral assignment of piperine **(21)**.

Position	Chemical shift (ppm)	
	Piperine	Compound 21
2	-	6.81 (d, *J* =15.0 Hz)
3	7.40 (ddd)	7.45 (ddd, *J* = 14.7 Hz, 8.5 Hz, 1.8 Hz)
4	6.76 (dd)	6.76 (dd, *J* =8.5 Hz, 15.0 Hz)
5	6.44 (d)	6.45 (d, *J* = 14.7 Hz)
7	6.77 (d)	6.82 (d, *J* = 8.0 Hz)
8	6.89 (dd)	6.87 (dd, *J* = 8.0 Hz, *J* = 1.6 Hz)
10 - OCH_2O	5.98 (s)	5.99 (s)
12	6.98 (d)	6.97 (d, *J* = 1.6 Hz)
13	3.52 (s)	3.58 (br s)
14	1.62 (m)	1.64 (m)
15	1.62 (m)	1.64 (m)
16	1.62 (m)	1.64 (m)
17	3.63 (s)	3.61 (br s)

3.2 Determination of the UV absorption of selected natural products

With certain natural products in hand, the measurement of the UV-absorbance of each compound to justify as UV-A and/or –B blocking agents and not absorbed at λ 311 nm was conducted using 8453 UV-Vis spectrophotometer. Individual spectrum was acquired in DMF with the concentration of 0.01% w/v. The ideal compound should absorb minimum absorbance at λ 311 nm, whereas it should exhibit large absorption in UV-A and/or –B region. The difference between absorbance at maximum wavelength (λ_{max}) and at the wavelength of 311 nm (λ_{311}) more than 1 was acceptable [39]. The UV spectra of selected compounds are presented in **Figures 3.10-3.13**. The UV spectral information of all twenty-one compounds is shown in **Table 3.8-3.9**.

Table 3.8 UV absorbance (a.u.), molar absorptivity (ε, $L.mol^{-1}.cm^{-1}$) and blocking agents group of selected natural products.

Compound (0.01% w/v)	λ_{max}			λ_{311}		Blocking agent group
	nm	Abs.	$\varepsilon x10^3$	Abs.	ε $x10^3$	
I. Commercial						
Baicalin **(1)**	280	3.9±0.1	19.7	3.1±0.0	15.6	NE
Berberine chloride hydrate **(2)**	280	4.0±0.0	20.0	2.0±0.0	10.1	UV-A &-B
Naringenin **(3)**	280	4.0±0.0	1.0	2.6±0.0	6.5	UV-B
Quercetin hydrate **(4)**	350	3.6±0.0	12.1	2.2±0.0	7.2	UV-A
Chrysin **(5)**	320	4.0±0.2	1.0	4.0±0.0	10.0	NE
Catechin **(6)**	280	1.6±0.0	5.3	0.05±0.0	0.1	UV-B
II. Supported by WC laboratory						
6,8-dibromochrysin **(7)**	300	3.8±0.1	19.2	2.8±0.0	13.8	NE
7-methoxy-coumarin **(8)**	311	4.0±0.0	13.3	4.0±0.0	13.3	NE
Phebalosin **(9)**	320	1.5±0.0	4.8	1.3±0.0	4.4	NE
Murrangatin acetate **(10)**	320	4.0±0.2	13.3	3.7±0.0	12.3	NE
Auraptene **(11)**	320	2.8±0.0	9.5	2.6±0.0	8.6	NE
Oxyresveratrol **(12)**	330	5.2±0.0	13.0	3.0±0.0	7.5	UV-A

Value, an average ± standard deviation of 3 replicates of the UV absorbance.

NE = non effective for delivered 311 nm into skin.

Table 3.9 UV absorbance (a.u.), molar absorptivity (ε, $L.mol^{-1}.cm^{-1}$) and blocking agents group of selected natural products (continued).

Compound 0.01% w/v	λ_{max}			λ_{311}		Blocking agents group
	nm.	Abs.	ε x10^3	Abs.	εx10^3	
III. **Extraction, isolation and purification**						
α-mangostin **(13)**	320	2.8±0.0	14.0	2.2±0.0	11.0	NE
Curcumin **(14)**	360	5.0±0.0	16,666.7	2.9±0.0	9.7	UV-A
Demethoxycurcumin **(15)**	280	3.4±0.0	11,333.3	1.5±0.0	5.0	UV-A &-B
Bis-demethoxycurcumin **(16)**	380	3.7±0.0	12,333.3	3.3±0.0	11.0	NE
Hesperidin **(17)**	290	2.1±0.0	7,000	0.49±0.0	1.6	UV-B
Hesperetin **(18)**	290	3.5±0.2	11,709.7	1.2±0.0	3.9	UV-B
Lutein **(19)**	400	3.5±0.3	17,542.0	1.5.±0.0	7.5	UV-B
Mansonone G **(20)**	280	3.6±0.0	9,000.0	0.4±0.0	1.0	UV-A&-B
Piperine **(21)**	340	4.0±0.1	13,333.3	3.9±0.1	13.1	NE

Value, an average ± standard deviation of 3 replicates of the UV absorbance.

NE = non effective for delivered 311 nm into skin.

From **Table 3.8**, four groups of compounds could be classified. The first group could absorb UV-A with weak absorption at λ 311 nm **(Figure 3.10).** Those compounds consist of quercetin hydrate **(4)**, oxyresveratrol **(12)** and curcumin **(14).** Their maximum wavelengths were not much different, but molar absorptivity was different. Quercetin hydrate **(4)** was a major flavonol possessing a carbonyl group at position 4, a double bond between carbons 2 and 3, and five hydroxyl groups at positions 3, 5, 7, 3′, 4. The non-bonding electrons from *o*-dihydroxy structure in ring C allowed easy electron delocalization of the internal hydrogen bonding.

Although oxyresveratrol **(12)** had equal conjugation of double bonds with quercetin hydrate **(4)** but it electron was more easily delocalized so it had more molar absorptivity than quercetin hydrate **(4)**.

Curcumin **(14)** had a chemical structure similar to dibenzoylmethane (UV-A chemical filter). The latter was a substituted diketone with a keto-enol tautomerism which confers the characteristics of UV-A filters (enol form). The keto form was responsible for higher maximum molar absorptivity than quercetin hydrate **(4)** and oxyresveratrol **(12)**.

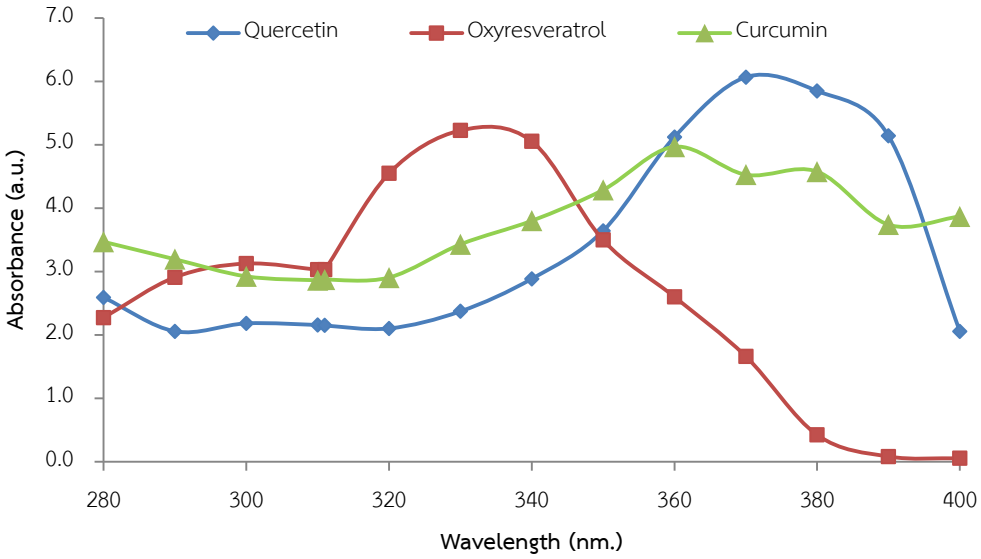

Figure 3.10 The UV spectra of collected samples in group I.

The second group could absorb UV-B with weak absorption at λ 311 nm **(Figure 3.11).** Naringenin **(3)**, catechin **(6),** hesperidin **(17),** hesperetin **(18)** and lutein **(19)** were in this category. Considering the maximum wavelength of UV-B blocking agents, the highest was found in lutein **(19),** followed by hesperetin **(18)** and naringenin **(3)** and not different for hesperidin **(17)** and catechin **(6).** Lutein **(19)** was naturally occurring carotenoids. The presence of ten conjugated double bonds (polyene chain) provided the highest maximum wavelength. In addition, the presence of two hydroxyl groups could donate back into ring C and made delocalization.

The maximum molar absorptivity was found to be higher than those for naringenin **(3)** and hesperetin **(18)**. Unfortunately, hesperidin **(17)** could not be used as UV blocking agent because it could not well dissolve in water.

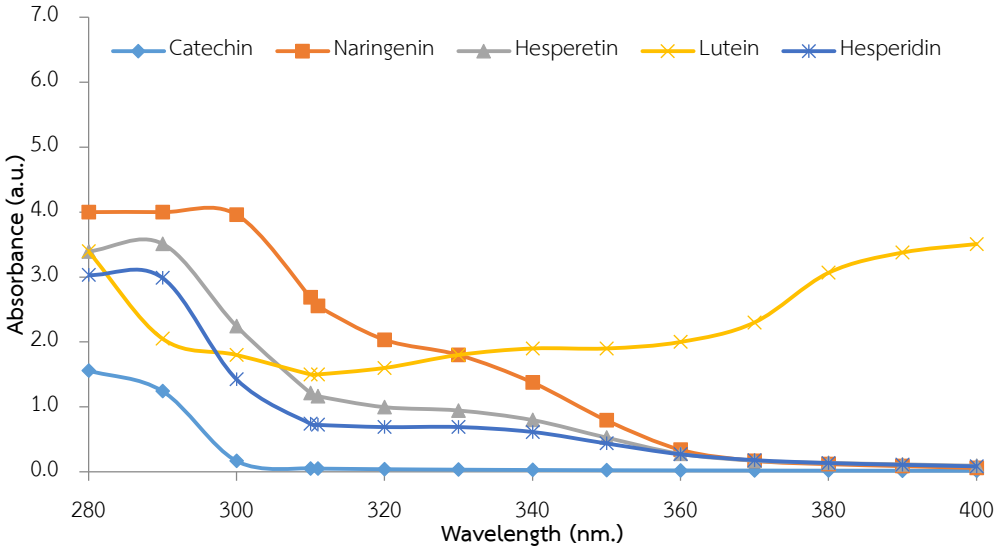

Figure 3.11 The UV spectra of collected samples in group II.

The next group could absorb both UV-A and –B while weakly absorbed at λ 311 nm **(Figure 3.12).** Those compounds were berberine chloride hydrate **(2)**, demethoxycurcumin **(15)** and mansonone G **(20)**. Their maximum wavelengths were similar, but found significant differentiation in the maximum molar absorptivity. Berberine chloride hydrate **(2)** was an isoquinoline alkaloid with the highest maximum molar absorptivity because of largest conjugation and auxochrome as dimethoxy and methylenedioxy groups. Demethoxycurcumin **(15)** had a UV-A chemical filter and responsible for higher in the maximum molar absorptivity than mansonone G **(20)** which was a structure of *o*-naphthoquinone. However, mansonone G **(20)** showed the lower absorption at narrow-band UV-B than demethoxycurcumin **(15)** and berberine chloride hydrate **(2)**, respectively.

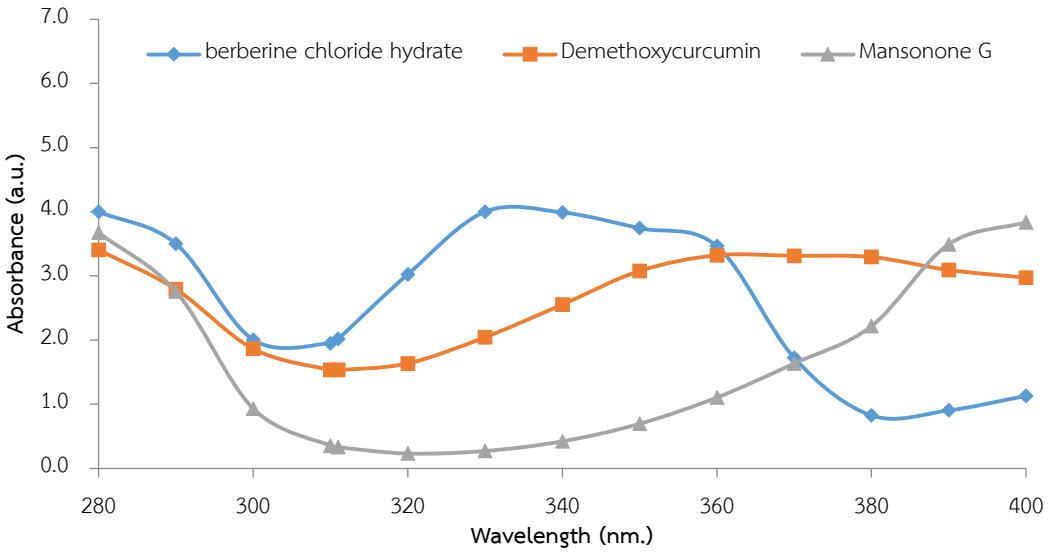

Figure 3 12 The UV spectra of collected samples in group III.

The non-effective blocking agents as the last group were those which did not absorb at λ 311 nm **(Figure 3.13).** It consisted of baicalin **(1),** chrysin **(5)**, 6,8-dibromochrysin **(7)**, 7-methoxy-8-(2'-methoxy-3'-hydroxy-3'-methylbutyl)coumarin **(8)**, phebalosin **(9),** murrangatin acetate **(10)**, auraptene **(11)**, α–mangostin **(13)**, bis-demethoxycurcumin **(16)** and piperine **(21).**

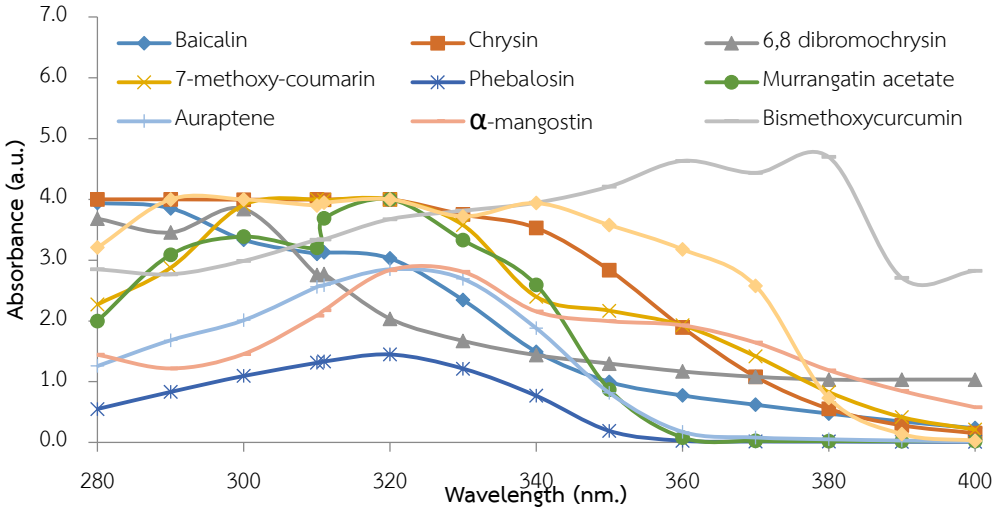

Figure 3 13 The UV spectra of collected samples in group IV.

In summary, it was disclosed that eleven natural products could deliver UV-light at λ 311 nm into skin. Among them, three, five and three compounds as UV-A, UV-B and both UV-A and -B blocking agents, respectively were selected for the next study.

3.3 Determination of the proper concentration of UV-blocking agents

The concentration of UV blocking agents was varied as 0.01, 0.005, 0.0025 and 0.001% w/v. The proper concentration of UV blocking agents was assumed to exhibit the absorbance at λ_{311} <1 and different from λ_{max} more than 1. The results are shown in **Figures 3.14-3.23.**

<u>Group I</u>

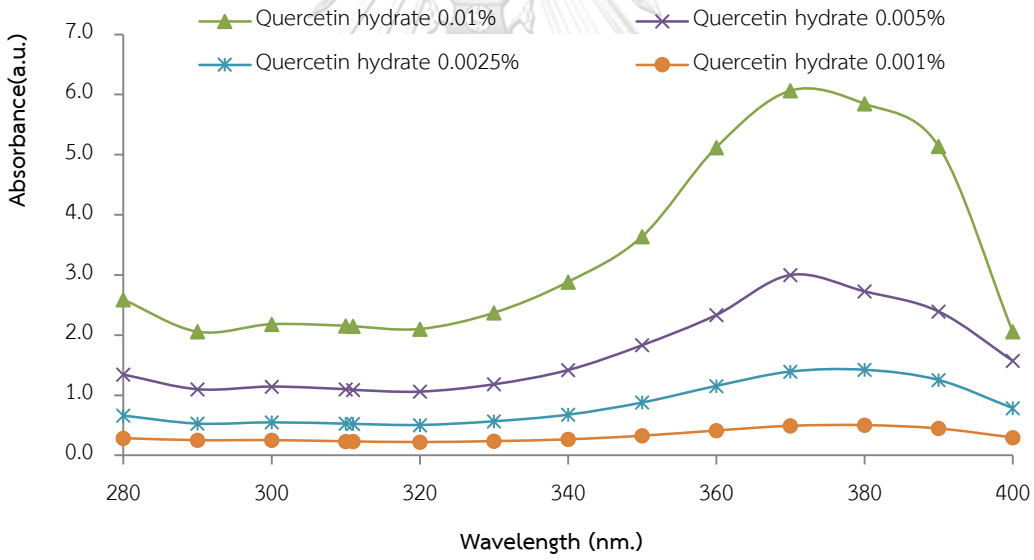

Figure 3.14 The UV spectra of quercetin hydrate **(4)** with various concentrations.

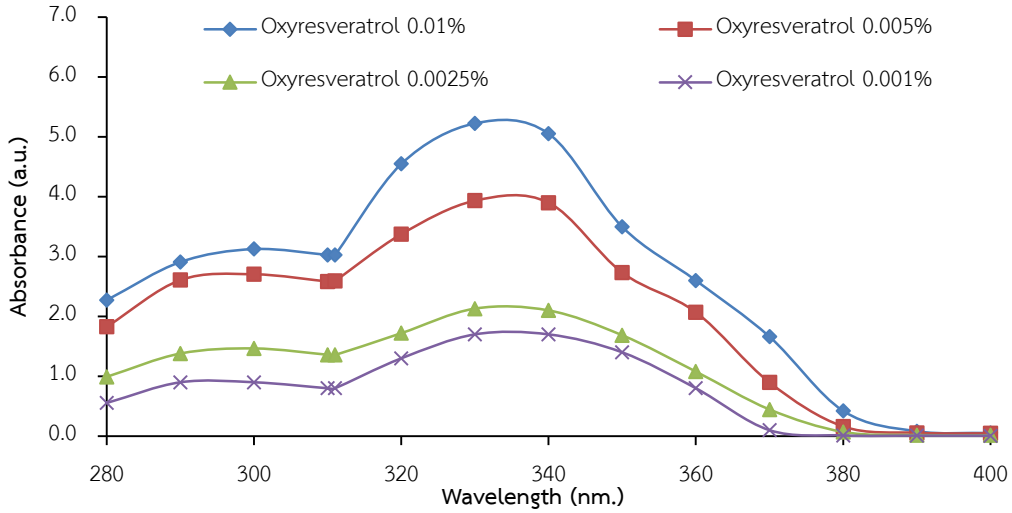

Figure 3.15 The UV spectra of oxyresveratrol **(12)** with various concentrations

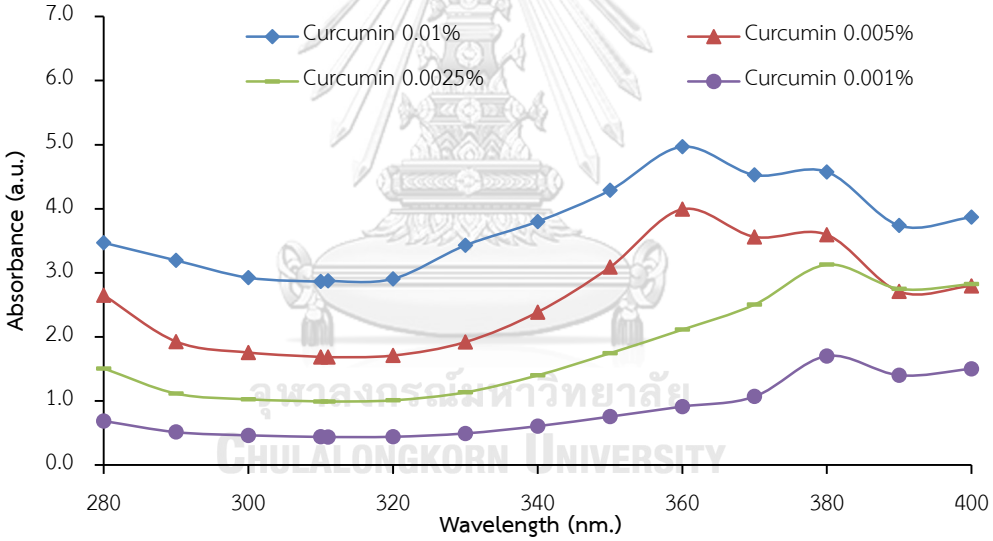

Figure 3.16 The UV spectra of curcumin **(14)** with various concentrations.

Group II

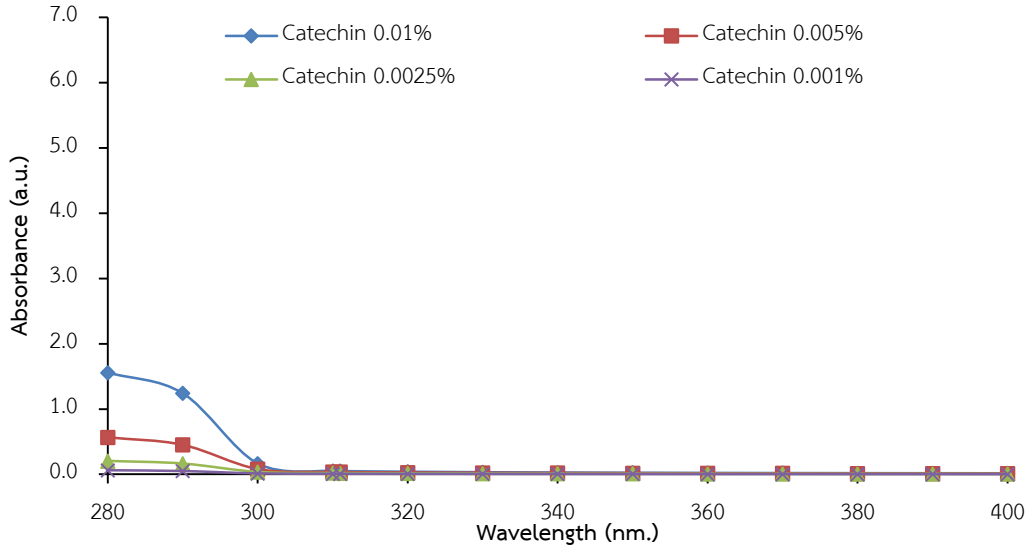

Figure 3.17 The UV spectra of catechin **(6)** with various concentrations

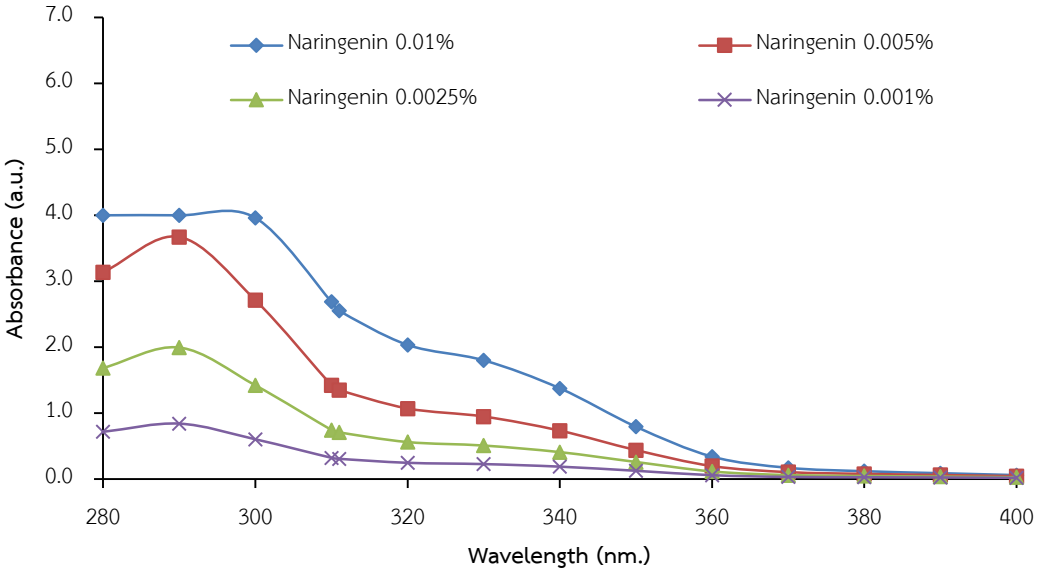

Figure 3.18 The UV spectra of naringenin (3) with various concentrations.

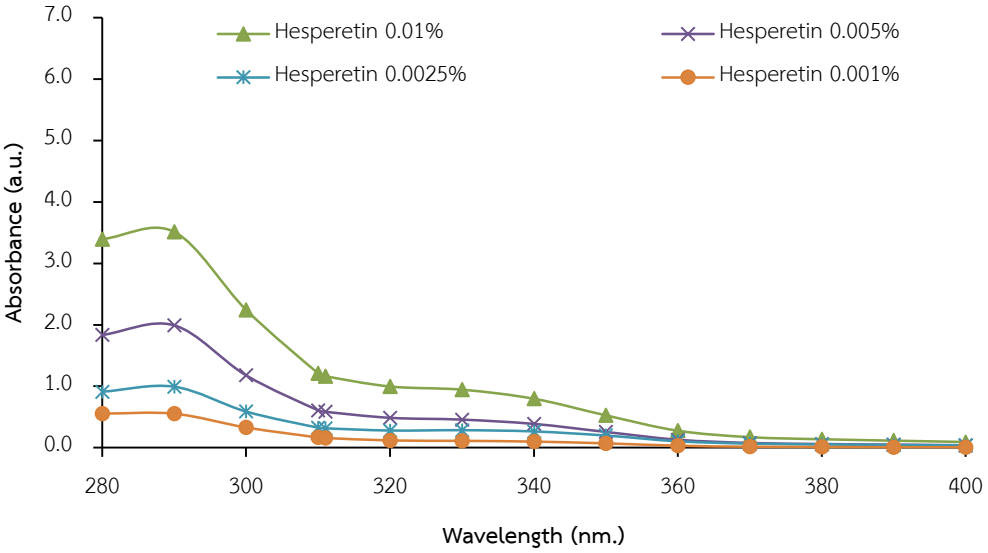

Figure 3.19 The UV spectra of hesperetin **(18)** with various concentrations.

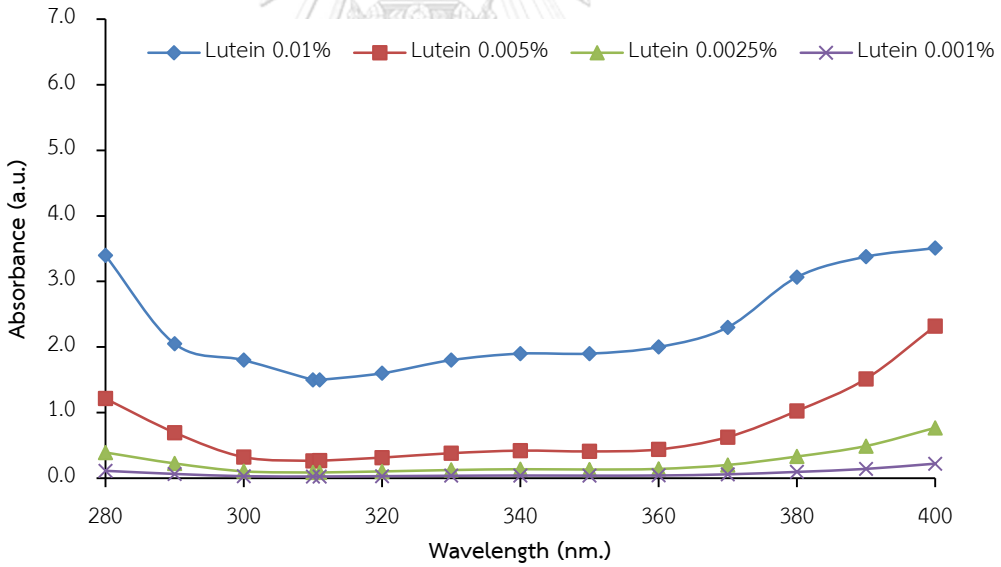

Figure 3.20 The UV spectra of lutein (19) with various concentrations.

Group III

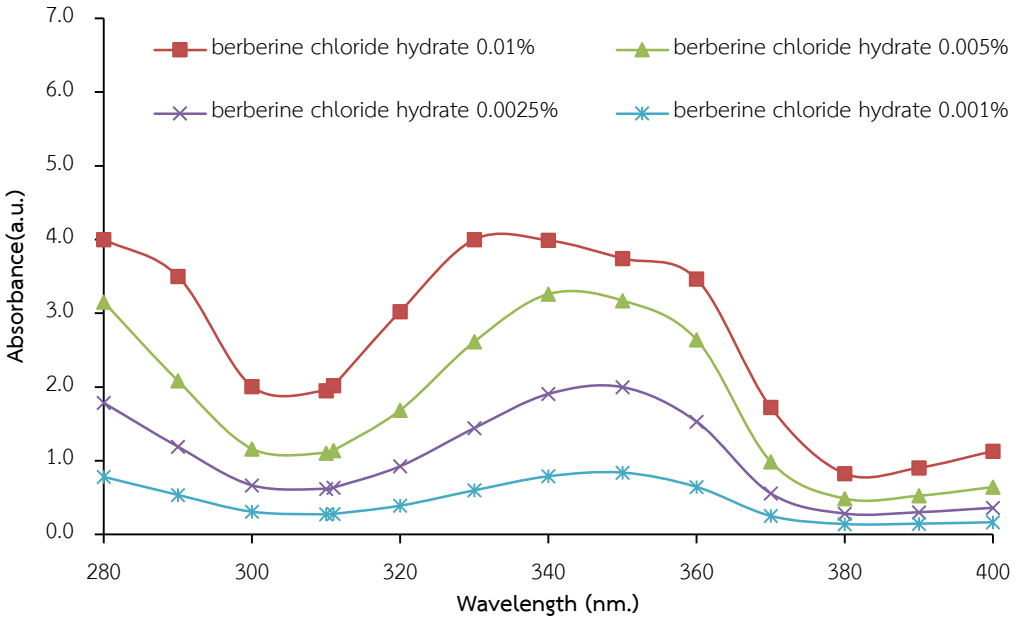

Figure 3.21 The UV spectra of berberine chloride hydrate **(2)** with various concentrations.

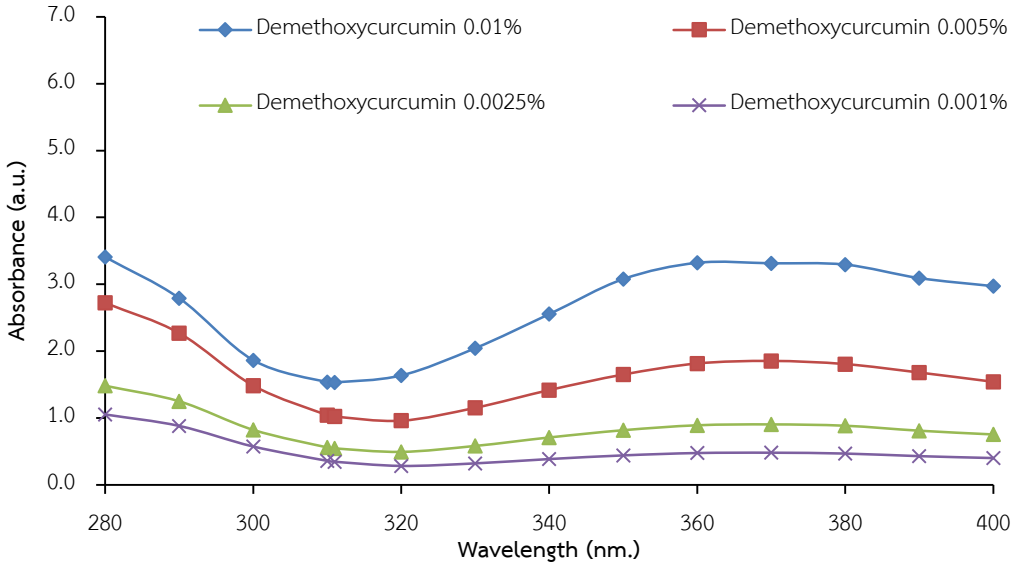

Figure 3.22 The UV spectra of demethoxycurcumin **(15)** with various concentrations.

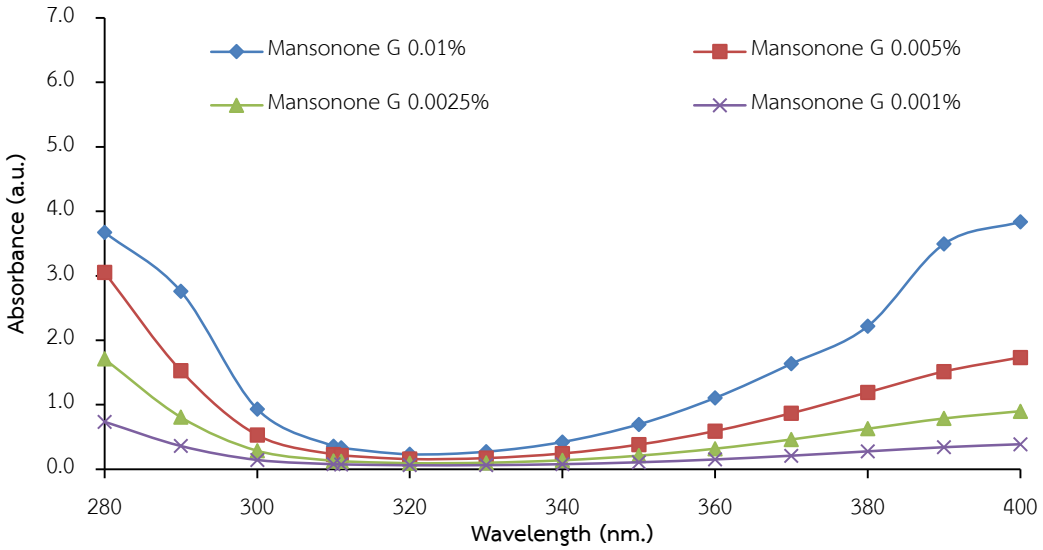

Figure 3.23 The UV spectra of mansonone G **(20)** with various concentrations.

From the above results, oxyresveratrol **(12)** and curcumin **(14)** had the optimal concentration at 0.0010% w/v. Quercetin hydrate **(4)**, berberine chloride hydrate **(2),** naringenin **(3)** and demethoxycurcumin **(15)** had the proper concentration at 0.0025% w/v while lutein **(19)** and hesperetin **(18)** expressed their suitable concentrations at 0.0050% w/v. The remained compounds revealed the suitable concentration to deliver narrow-band UV-B at 0.0100% w/v. The summary of the proper concentration of UV blocking agents is shown in **Table 3.10**.

Table 3.10 Summary of the proper concentration of UV blocking agents.

Compound	Concentration (%w/v)	λ_{max}		λ_{311}
		nm.	Abs	Abs
Group I				
Quercetin hydrate **(4)**	0.0025	380	1.4±0.0	0.5±0.0
Oxyresveratrol **(12)**	0.0010	330	1.7±0.0	0.8±0.0
Curcumin **(14)**	0.0010	380	1.7±0.0	0.4±0.0
Group II				
Naringenin **(3)**	0.0025	290	2.0±0.0	0.7±0.0
Catechin **(6)**	0.0100	280	1.6±0.0	0.05±0.0
Hesperetin **(18)**	0.0050	290	1.8±0.0	0.6±0.0
Lutein **(19)**	0.0050	400	2.3±0.2	0.3±0.0
Group III				
Berberine chloride hydrate **(2)**	0.0025	350	2.0±0.0	0.6±0.0
Demethoxycurcumin **(15)**	0.0025	280	1.5±0.0	0.5±0.0
Mansonone G **(20)**	0.0100	400	3.8±0.0	0.3±0.0

Value, an average ± standard deviation of 3 replicates of the UV absorbance.

For the compounds in group I, curcumin **(14)** was the lowest absorbed at λ 311 nm. However quercetin hydrate **(4)** was selected for further study because it had the most effective bandwidth**.** For group II, naringenin **(3)**, catechin **(6)** and hesperetin **(18)** had equal effective bandwidth while lutein **(19)** expressed the lowest bandwidth. Nonetheless, this research focuses on the delivery of narrow-band UV-B to skin, so catechin **(6)** was selected as a UV-B blocking agent. Considering for group III, berberine chloride hydrate **(2)** exhibited the lowest effective bandwidth at UV-B range but higher than mansonone G **(20)** in UV-A range. Demethoxycurcumin **(15)** displayed the highest effective bandwidth in UV-A range while mansonone G **(20)** showed the highest in UV-B range. However, the latter was selected because it displayed the lowest absorbance at λ 311 nm.

Nowadays there is no UV blocking agents that allow only λ 311 nm pass through and at the same time absorb UV-A and –B. The attempt for the next step is trying to combine UV-A blocking agent (quercetin hydrate **(4)**) with UV-B blocking agent (catechin **(6)**) and UV-A and –B (mansonone G **(20)**). The justification for the best couple would base on the combination that could well-absorb UV-A and –B, but less absorbed in narrow-band UV-B region.

3.4 The investigation on the combination of blocking agents.

After the optimal concentration of selected compounds was determined, another attempt to combine blocking agents was performed with the aim to search for the most proper mixture that could highly absorb UV-A and –B regions, at the same time with minimum absorption at λ 311 nm. The combination was carried out by mixing UV-A and UV-B blocking agents 1:1 ratio (5:5 mL). Three possible combinations of blocking agents: UV-A blocking agent (quercetin hydrate **(4)**) with UV-B blocking agents (catechin **(6)**) and UV-A and –B (mansonone G **(20)**) is shown in **Figure 3.24.** The UV absorbance of the combination of selected natural products is presented in **Table 3.11**.

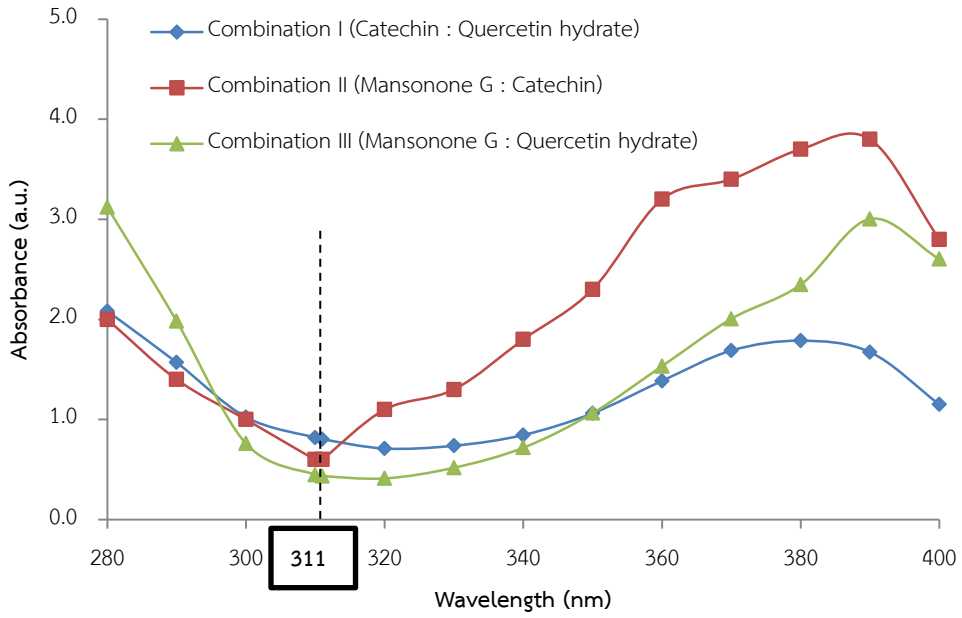

Figure 3.24 The UV spectra of the combination of selected natural products.

Table 3.11 The UV absorbance of the random combination.

Combination		λ_{max}		λ_{311}
UV-B	**UV-A**	**nm**	**Abs**	**Abs**
I. Catechin (16) 0.01% w/v	**Quercetin hydrate (4)** 0.005 %w/v	280,380	2.1±0.0, 1.8±0.0	0.8±0.0
II. Catechin (16) 0.01% w/v	**Mansonone G (20)** 0.01% w/v	280,390	2.0±0.0, 3.8±0.0	0.6±0.0
III. Mansonone G (20) 0.01% w/v	**Quercetin hydrate (4)** 0.0025 %w/v	280,390	3.1±0.0, 3.0±0.0	0.4±0.0

Value, an average ± standard deviation of 3 replicates of the UV absorbance.

Focusing on the minimum absorbance at narrow-band UV-B, it was found that combination III displayed the best result since it revealed the lowest absorption at λ 311 nm. From the previous study [40], DHHB combined with α-GH gave the absorbance around 0.6 a.u. Thus, the combination of quercetin hydrate **(4)** and mansonone G **(20)** revealed better results. It should be noted here that there was no report on the use of quercetin hydrate **(4)** and mansonone G **(20)** as UV-A and/or UV-B blocking agents and the combination of these natural products for psoriasis phototherapy. However, this combination needs further examination for cytotoxicity and photostability.

3.5 Cytotoxicity and photostability tests

3.5.1 Cytotoxicity test

The cytotoxic effect of the combination of UV blocking agents was evaluated using HaCaT cells, a rapid multiplying human keratinocyte cell line model of epidermal hyperproliferation in psoriasis. The %cell viability results derived from the tested UV blocking agent combination were considered for the safety of the mixture upon exposure to HaCaT cell. The combination of avobenzone and octinoxate (AO) at the ratio of 1:3.75 was used as positive control. **Figure 3.25** shows that the cell survival of

quercetin hydrate **(4)** combined with mansonone G **(20)** (QM) was lower than positive control and tended to decrease with higher concentration than 10 µg/mL.

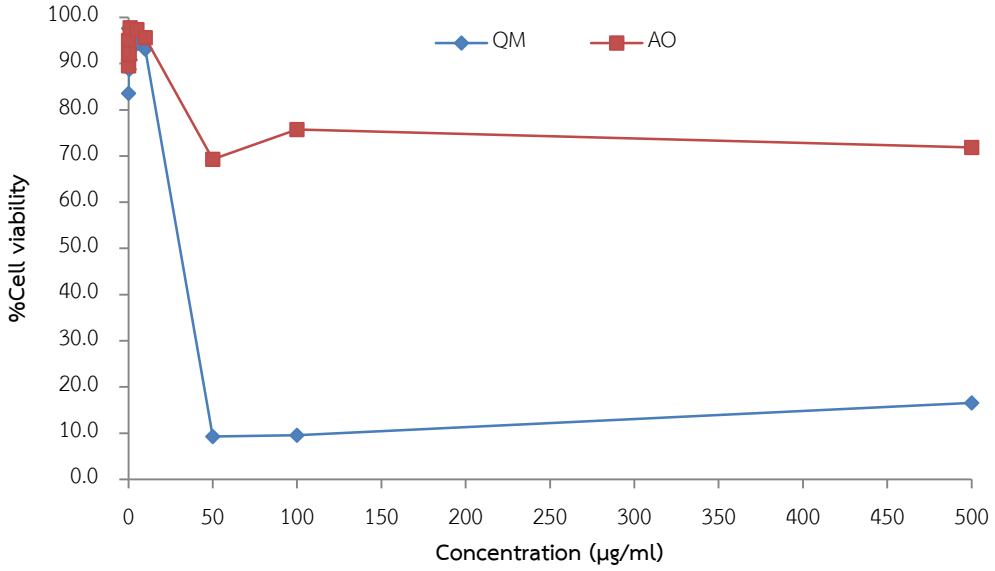

Figure 3.25 % Cell viability of UV blocking agent combination.

These results were validated using the combination of avobenzone and octinoxate. From the previous study [86], the combined AO revealed more IC_{50} than avobenzone or octinoxate alone. Thus, the combination of AO could be used as positive control. Compared with the combination of QM and AO, it was found that the combination of QM was more toxic than that of AO at high concentration, but not different at low concentration.

3.5.2 Photostability

The ideal effective topical cream should contain stable active ingredients. Thus, the photostability of the combination between quercetin hydrate **(4)** 0.0025 %w/v and mansonone G **(20)** 0.01 %w/v was evaluated. Six sets of the combination were prepared: one was kept in the dark for 60 min, four samples were exposed to sunlight for 5, 15, 30, and 60 min and the other was irradiated by Solar stimulator for 60 min. The UV spectra of all samples after examination for specific duration were recorded and the results are presented in **Figure 3.26** and **Table 3.1**3

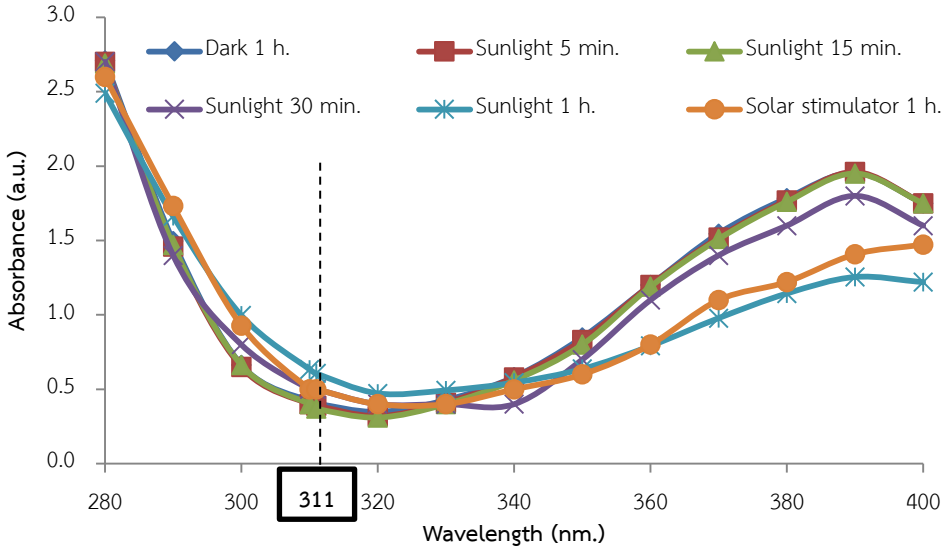

Figure 3.26 The UV spectra of the combination of QM under the conditions in dark, exposure with sunlight and solar stimulator.

Table 3.12 The UV absorbance of the combination of QM under different conditions.

Condition	λ_{max}		λ_{311}
	nm	Abs	Abs
Dark	280	2.7±0.0	0.4±0.0
Sunlight 5 min	280	2.7±0.0	0.4±0.0
Sunlight 15 min	280	2.7±0.0	0.4±0.0
Sunlight 30 min	280	2.7±0.0	0.4±0.0
Sunlight 60 min	280	2.5±0.0	0.6±0.0
Solar stimulator 60 min	280	2.6±0.0	0.5±0.0

From the results in Figure 3.26, it was found that after exposure to the sunlight and the light from solar stimulator for 60 min, the absorbance at λ 311 nm tended to increase. This implied lower delivery of the light intensity at λ 311 nm into skin. Compared the absorbance at λ 311 nm of sunlight and light from solar stimulator, the results were not different. This clearly indicated that the exposure time when using this combination should not over 60 min. However, in practice the patients were

normally exposed with the λ 311 nm light no longer than 10 min [97]. After QM was exposed with light, the quantitative analysis of both active ingredients (quercetin hydrate **(4)** and mansonone G **(20)** was conducted and the results are collected in **Table 3.13.**

Table 3.13 The quantity of active ingredients (QM) under various conditions.

Conditions	Quercetin hydrate **(4)** (% w/v)	%Diff	Mansonone G **(20)** (% w/v)	%Diff
Dark 60 min	0.0025	0.0	0.0067	0.0
Sunlight 5 min	0.0025	0.0	0.0067	0.0
Sunlight 15 min	0.0025	0.0	0.0067	0.0
Sunlight 30 min	0.0023	0.0	0.0067	0.0
Sunlight 60 min	0.0017	32.0	0.0062	7.5
Solar stimulator 60 min	0.0018	28.0	0.0064	4.5

%Difference = [(%w/v at dark - %wlv at others condition)/ %w/v at dark]*100%

From **Table 3.13**, quercetin hydrate **(4)** was decreased by 28 and 32% when exposed to light from solar stimulator and sunlight, respectively. For mansonone G **(20)** was decreased only 4.5-7.5% upon exposure to solar stimulator and sunlight, respectively. This indicated that if quercetin hydrate **(4)** decreased, the absorption at λ 311 nm tended to increase together. In summary, these two compounds could expose with light no longer than 30 min.

3.6 Formulation of the topical cream containing UV-A and –B blocking agents.

Topical cream was kindly prepared by pharmacy government unit at Chulalongkorn Hospital. The cold cream was selected as the topical cream from satisfaction of the patients. The topical cream containing these two active ingredients was yellow with no problem of dissolving in formulation process. The topical cream containing QM is shown in **Figure 3.27.**

Figure 3. 27 The topical cream containing the combination between mansonone G **(20)** and quercetin hydrate **(4).**

CHAPTER IV

CONCLUSION

Many natural compounds were disclosed to reveal strong absorption in UV-A and UV-B. But this research interested in weak absorption at narrow-band UV-B and strongly at UV-A and UV-B. With the assumption of the difference between absorbance at λ max and λ 311 more than 1 a.u. Quercetin hydrate (**4**) 0.0025% w/v and mansonone G (**20**) were selected as a composition for the topical cream. However, the best combination should be safe for human skin so the cytotoxicity was evaluated on combination of QM to keratinocyte cultures compared with AO combination. The toxic of QM occurred at the high concentration. Photostability of the combination found that if quercetin hydrate **(4)** decreased, the absorption at λ 311 nm tended to increase together. Thus, the two compounds should be exposed to light no longer than 30 min. The topical cream containing QM was formulated under cold base cream, and it gave yellow color.

Suggestion for future work

The topical cream containing mansonone G and quercetin hydrate will be evaluated for SPF value for confirmation of delivery at λ 311 nm and efficacy on the psoriasis patient also. If it is successful, the combination should provide a more convenient way to deliver narrow-band UV-B phototherapy for patients.

REFERENCES

1. Rácz, E. and E.P. Prens, *Molecular pathophysiology of psoriasis and molecular targets of antipsoriatic therapy.* Expert reviews in molecular medicine, 2009. **11**.
2. Aberer, W., et al., *Ultraviolet light depletes surface markers of Langerhans cells.* Journal of Investigative Dermatology, 1981. **76**(3): p. 202-210.
3. Halliday, G.M. and S. Rana, *Waveband and Dose Dependency of Sunlight-induced Immunomodulation and Cellular Changes.* Photochemistry and photobiology, 2008. **84**(1): p. 35-46.
4. Halverstam, C.P. and M. Lebwohl, *Nonstandard and off-label therapies for psoriasis.* Clinics in dermatology, 2008. **26**(5): p. 546-553.
5. Bonis, B., et al., *308 nm UVB excimer laser for psoriasis.* The Lancet, 1997. **350**(9090): p. 1522.
6. Fischer, T., J. Alsins, and B. Berne, *Ultraviolet-action Spectrum and Evaluation of Ultraviolet Lamps for Psoriasis Healing.* International journal of dermatology, 1984. **23**(10): p. 633-637.
7. Parrish, J.A. and K.F. Jaenicke, *Action spectrum for phototherapy of psoriasis.* Journal of Investigative Dermatology, 1981. **76**(5): p. 359-362.
8. Coven, T.R., et al., *Narrowband UV-B produces superior clinical and histopathological resolution of moderate-to-severe psoriasis in patients compared with broadband UV-B2.* Archives of dermatology, 1997. **133**(12): p. 1514-1522.
9. Walters, I.B., et al., *Suberythemogenic narrow-band UVB is markedly more effective than conventional UVB in treatment of psoriasis vulgaris.* Journal of the American Academy of Dermatology, 1999. **40**(6): p. 893-900.
10. Picot, E., et al., *Treatment of psoriasis with a 311-nm UVB lamp.* British Journal of Dermatology, 1992. **127**(5): p. 509-512.

11. Storbeck, K., et al., *Narrow-band UVB (311 nm) versus conventional broad-band UVB with and without dithranol in phototherapy for psoriasis.* Journal of the American Academy of Dermatology, 1993. **28**(2): p. 227-231.
12. GREEN, C., et al., *311 nm UVB phototherapy—an effective treatment for psoriasis.* British Journal of Dermatology, 1988. **119**(6): p. 691-696.
13. Larkö, O., *Treatment of psoriasis with a new UVB-lamp.* Acta dermato-venereologica, 1989. **69**(4): p. 357-359.
14. Murase, J.E., et al., *Hormonal effect on psoriasis in pregnancy and post partum.* Archives of Dermatology, 2005. **141**(5): p. 601-606.
15. Stern, R.S., *Psoralen and ultraviolet a light therapy for psoriasis.* New England Journal of Medicine, 2007. **357**(7): p. 682-690.
16. Schmitt, J., et al., *Efficacy and tolerability of biologic and nonbiologic systemic treatments for moderate-to-severe psoriasis: meta-analysis of randomized controlled trials.* British Journal of Dermatology, 2008. **159**(3): p. 513-526.
17. Gerber, W., et al., *Ultraviolet B 308-nm excimer laser treatment of psoriasis: a new phototherapeutic approach.* British Journal of Dermatology, 2003. **149**(6): p. 1250-1258.
18. El-Ghorr, A.A. and M. Norval, *Biological effects of narrow-band (311 nm TL01) UVB irradiation: a review.* Journal of Photochemistry and Photobiology B: Biology, 1997. **38**(2): p. 99-106.
19. Gibbs, N.K., et al., *The phototumorigenic potential of broad-band (270–350 nm) and narrow-band (311–313 nm) phototherapy sources cannot be predicted by their edematogenic potential in hairless mouse skin.* Journal of investigative dermatology, 1995. **104**(3): p. 359-363.
20. Weischer, M., et al., *No evidence for increased skin cancer risk in psoriasis patients treated with broadband or narrowband UVB phototherapy: a first retrospective study.* Acta dermato-venereologica, 2004. **84**(5).
21. Hearn, R., et al., *Incidence of skin cancers in 3867 patients treated with narrow-band ultraviolet B phototherapy.* British Journal of Dermatology, 2008. **159**(4): p. 931-935.

22. Man, I., et al., *The photocarcinogenic risk of narrowband UVB (TL-01) phototherapy: early follow-up data.* British Journal of Dermatology, 2005. **152**(4): p. 755-757.

23. Black, R. and A. Gavin, *Photocarcinogenic risk of narrowband ultraviolet B (TL-01) phototherapy: early follow-up data.* British Journal of Dermatology, 2006. **154**(3): p. 566-567.

24. Choi, C., et al., *The effect of narrowband ultraviolet B on the expression of matrix metalloproteinase-1, transforming growth factor-β1 and type I collagen in human skin fibroblasts.* Clinical and experimental dermatology, 2007. **32**(2): p. 180-185.

25. Krueger, J.G., et al., *Successful ultraviolet B treatment of psoriasis is accompanied by a reversal of keratinocyte pathology and by selective depletion of intraepidermal T cells.* Journal of Experimental Medicine, 1995. **182**(6): p. 2057-2068.

26. Carrascosa, J.M., et al., *Effects of narrowband UV-B on pharmacodynamic markers of response to therapy: an immunohistochemical study over sequential samples.* Journal of cutaneous pathology, 2007. **34**(10): p. 769-776.

27. Ozawa, M., et al., *312-nanometer ultraviolet B light (narrow-band UVB) induces apoptosis of T cells within psoriatic lesions.* Journal of experimental medicine, 1999. **189**(4): p. 711-718.

28. Walters, I.B., et al., *Narrowband (312-nm) UV-B suppresses interferon γ and interleukin (IL) 12 and increases IL-4 transcripts: differential regulation of cytokines at the single-cell level.* Archives of dermatology, 2003. **139**(2): p. 155-161.

29. Gutierrez-Steil, C., et al., *Sunlight-induced basal cell carcinoma tumor cells and ultraviolet-B-irradiated psoriatic plaques express Fas ligand (CD95L).* Journal of Clinical Investigation, 1998. **101**(1): p. 33.

30. Piskin, G., et al., *Ultraviolet-B irradiation decreases IFN-γ and increases IL-4 expression in psoriatic lesional skin in situ and in cultured dermal T cells derived from these lesions.* Experimental dermatology, 2003. **12**(2): p. 172-180.

31. Piskin, G., et al., *T cells in psoriatic lesional skin that survive conventional therapy with NB-UVB radiation display reduced IFN-γ expression.* Archives of dermatological research, 2004. **295**(12): p. 509-516.
32. Piskin, G., et al., *IL-4 expression by neutrophils in psoriasis lesional skin upon high-dose UVB exposure.* Dermatology, 2003. **207**(1): p. 51-53.
33. DeSilva, B., et al., *Local effects of TL01 phototherapy in psoriasis.* Photodermatology, photoimmunology & photomedicine, 2008. **24**(5): p. 268-269.
34. Pacheco-Palencia, L.A., et al., *Protective effects of standardized pomegranate (Punica granatum L.) polyphenolic extract in ultraviolet-irradiated human skin fibroblasts.* Journal of agricultural and food chemistry, 2008. **56**(18): p. 8434-8441.
35. Jivaramonaikul, W., P. Rashatasakhon, and S. Wanichwecharungruang, *UVA absorption and photostability of coumarins.* Photochemical & Photobiological Sciences, 2010. **9**(8): p. 1120-1125.
36. Korać, R.R. and K.M. Khambholja, *Potential of herbs in skin protection from ultraviolet radiation.* Pharmacognosy reviews, 2011. **5**(10): p. 164.
37. Manasathien, J., K. Indrapichate, and K. Intarapichet, *Antioxidant activity and bioefficacy of pomegranate Punica granatum Linn. peel and seed extracts.* Global Journal of Pharmacology, 2012. **6**(2): p. 131-141.
38. Goswami, P.K., M. Samant, and R. Srivastava, *Natural sunscreen agents: A review.* SAJP, 2013. **2**: p. 458-463.
39. Goren, A., et al., *Novel topical cream delivers safe and effective alternative to traditional psoriasis phototherapy.* Dermatologic therapy, 2014. **27**(5): p. 260-263.
40. McCoy, J., A. Goren, and T. Lotti, *In vitro evaluation of a novel topical cream for vitiligo and psoriasis that selectively delivers NB-UVB therapy when exposed to sunlight.* Dermatologic therapy, 2014. **27**(2): p. 117-120.
41. Rojas, J., C. Londoño, and Y. Ciro, *The health benefits of natural skin uva photoprotective compounds found in botanical sources*. Vol. 8. 2016. 13-23.

42. Saraf, S. and C. Kaur, *Phytoconstituents as photoprotective novel cosmetic formulations.* Pharmacognosy reviews, 2010. **4**(7): p. 1.
43. Hupel, M., N. Poupart, and E.A. Gall, *Development of a new in vitro method to evaluate the photoprotective sunscreen activity of plant extracts against high UV-B radiation.* Talanta, 2011. **86**: p. 362-371.
44. Angelo, G., et al., *Biochemical composition and antioxidant properties of Lavandula angustifolia Miller essential oil are shielded by propolis against UV radiations.* Photochemistry and photobiology, 2014. **90**(3): p. 702-708.
45. Nascimento, C.S., et al., *Incremento do FPS em formulação de protetor solar utilizando extratos de própolis verde e vermelha.* Revista Brasileira de Farmácia, 2009. **30**(1): p. 334-339.
46. Nichols, J.A. and S.K. Katiyar, *Skin photoprotection by natural polyphenols: anti-inflammatory, antioxidant and DNA repair mechanisms.* Archives of dermatological research, 2010. **302**(2): p. 71-83.
47. Vaid, M. and S.K. Katiyar, *Molecular mechanisms of inhibition of photocarcinogenesis by silymarin, a phytochemical from milk thistle (Silybum marianum L. Gaertn.).* International journal of oncology, 2010. **36**(5): p. 1053-1060.
48. Korkina, L., *Phenylpropanoids as naturally occurring antioxidants: from plant defense to human health.* Cell Mol Biol, 2007. **53**(1): p. 15-25.
49. Kowalski, R. and T. Wolski, *Evaluation of phenolic acid content in Silphium perfoliatum L. leaves, inflorescences and rhizomes.* Electronic Journal of Polish Agricultural Universities, 2003. **6**(1).
50. Butnariu, M.V. and C.V. Giuchici, *The use of some nanoemulsions based on aqueous propolis and lycopene extract in the skin's protective mechanisms against UVA radiation.* Journal of nanobiotechnology, 2011. **9**(1): p. 3.
51. Acevedo, J.A., et al., *Photoprotective activity of Buddleja scordioides.* Fitoterapia, 2005. **76**(3): p. 301-309.
52. Mabry, T., K. Markham, and M. Thomas. *The systematic identification of flavonoids. 1970*. in *Library of Congress Catalog Card*.

53. Timbola, A.K., et al., *Electrochemical oxidation of quercetin in hydro-alcoholic solution.* Journal of the Brazilian Chemical Society, 2006. **17**(1): p. 139-148.
54. Yamuna, J. and N. Athony, *Citrus sinensis L. leaf extract as an efficient green corrosion inhibitor for mild steel in aqueous medium.* International Journal of Chem. Tech. Research, 2014. **7**(01): p. 37-43.
55. Souza, C.M.P.d., *Opuntia ficus-indica (L) Mill.: caracterização fisico-química e avaliação do efeito antioxidante, antibacteriano, fotoprotetor e inibidor da tirosinase.* 2012.
56. Semerdjieva, S., et al., *Contrasting strategies for UV-B screening in sub-Arctic dwarf shrubs.* Plant, cell & environment, 2003. **26**(6): p. 957-964.
57. Cao, Y., et al., *Analysis of flavonoids in Ginkgo biloba L. and its phytopharmaceuticals by capillary electrophoresis with electrochemical detection.* Anal Bioanal Chem, 2002. **374**(2): p. 294-9.
58. Patil, S., et al., *Formulation of gel and its UV protective study of some medicinal flowers.* Asian J. Pharm. Ana, 2011. **1**(2): p. 34-35.
59. GARCÍA-BORES, A.M., et al., *Photoprotective activity of Yucca periculosa polyphenols.* Boletín Latinoamericano y del Caribe de Plantas Medicinales y Aromáticas, 2010. **9**(2).
60. Tan, J., *Dietary isoflavones: aglycones and glycosides*. 2011: University of Leeds.
61. Choquenet, B., et al., *Quercetin and rutin as potential sunscreen agents: determination of efficacy by an in vitro method.* Journal of natural products, 2008. **71**(6): p. 1117-1118.
62. Silva, C.G., et al., *Photochemical and photocatalytic degradation of trans-resveratrol.* Photochemical & Photobiological Sciences, 2013. **12**(4): p. 638-644.
63. Wu, N.-L., et al., *Chrysin protects epidermal keratinocytes from UVA-and UVB-induced damage.* Journal of agricultural and food chemistry, 2011. **59**(15): p. 8391-8400.
64. Moin, A.M., et al., *Validated method for silymarin by spectrophotometry in bulk drug and pharmaceutical formulations.* Journal of Chemical and Pharmaceutical Research, 2010. **2**(1): p. 396-400.

65. Couteau, C., et al., *Silymarin, a molecule of interest for topical photoprotection.* Natural product research, 2012. **26**(23): p. 2211-2214.
66. Katiyar, S.K., *Silymarin and skin cancer prevention: anti-inflammatory, antioxidant and immunomodulatory effects.* International journal of oncology, 2005. **26**(1): p. 169-176.
67. Srilatha, D., et al., *Development and validation of UV spectrophotometric method for simultaneous estimation of hesperidin and diosmin in the pharmaceutical dosage form.* ISRN Spectroscopy, 2013. **2013**.
68. SATO, A., Y. HAYAsHI, and K. KITAO, *Studies on Wood Phenolics (III): Identification of Sakuranetin from Wood of Haplormosia monophylla HARMS (Leguminosae).* 1968.
69. César, I.d.C., et al., *Quantitation of genistein and genistin in soy dry extracts by UV-Visible spectrophotometric method.* Química Nova, 2008. **31**(8): p. 1933-1936.
70. Scarmo, S., et al., *Significant correlations of dermal total carotenoids and dermal lycopene with their respective plasma levels in healthy adults.* Archives of biochemistry and biophysics, 2010. **504**(1): p. 34-39.
71. Zanatta, C., et al., *Photoprotective potential of emulsions formulated with Buriti oil (Mauritia flexuosa) against UV irradiation on keratinocytes and fibroblasts cell lines.* Food and chemical Toxicology, 2010. **48**(1): p. 70-75.
72. Aust, O., et al., *Supplementation with tomato-based products increases lycopene, phytofluene, and phytoene levels in human serum and protects against UV-light-induced erythema.* International journal for vitamin and nutrition research, 2005. **75**(1): p. 54-60.
73. Trevithick-Sutton, C.C., et al., *The retinal carotenoids zeaxanthin and lutein scavenge superoxide and hydroxyl radicals: a chemiluminescence and ESR study.* Mol Vis, 2006. **12**(12): p. 1127-35.
74. Navarro-Martínez, M.D., F. García-Cánovas, and J.N. Rodríguez-López, *Tea polyphenol epigallocatechin-3-gallate inhibits ergosterol synthesis by disturbing folic acid metabolism in Candida albicans.* Journal of Antimicrobial Chemotherapy, 2006. **57**(6): p. 1083-1092.

75. Nagarajan, S., et al., *Biocatalytically oligomerized epicatechin with potent and specific anti-proliferative activity for human breast cancer cells.* Molecules, 2008. **13**(11): p. 2704-2716.

76. Weber, H.A., et al., *Comparison of proanthocyanidins in commercial antioxidants: grape seed and pine bark extracts.* Journal of agricultural and food chemistry, 2007. **55**(1): p. 148-156.

77. Fu, C., et al., *Structure, antioxidant and α-amylase inhibitory activities of longan pericarp proanthocyanidins.* Journal of Functional Foods, 2015. **14**: p. 23-32.

78. Vergara, C., et al., *Anthocyanins that confer characteristic color to red copihue flowers (Lapageria rosea).* Journal of the Chilean Chemical Society, 2009. **54**(2): p. 194-197.

79. Lopes-da-Silva, M., M. Escribano-Bailón, and C. Santos-Buelga, *Stability of pelargonidin 3-glucoside in model solutions in the presence and absence of flavanols.* American Journal of Food Technology, 2007: p. 602-617.

80. Burdulis, D., et al., *Study of diversity of anthocyanin composition in bilberry (Vaccinium myrtillus L.) fruits.* Medicina, 2007. **43**(12): p. 971-977.

81. Spagnol, C.M., et al., *Validation of Caffeic Acid in Emulsion by UV-Spectrophotometric Method.* Physical Chemistry, 2015. **5**(1): p. 16-22.

82. Holser, R.A., *Principal component analysis of phenolic acid spectra.* ISRN Spectroscopy, 2012. **2012**.

83. Phatak, S.V. and M.R. Heble, *Rosmarinic Acid Synthesis in Shoot Cultures of Mentha arvensis Linn.* 2002.

84. Saratha, V., S.I. Pillai, and S. Subramanian, *Isolation and characterization of lupeol, a triterpenoid from Calotropis gigantea latex.* International Journal of Pharmaceutical Sciences Review and Research, 2011. **10**(2): p. 54-56.

85. Sri, N.U., et al., *FT-IR, FT-Raman and UV–Vis spectra and DFT calculations of 3-cyano-4-methylcoumarin.* Spectrochimica Acta Part A: Molecular and Biomolecular Spectroscopy, 2012. **97**: p. 728-736.

86. Hayden, C., et al., *Sunscreen penetration of human skin and related keratinocyte toxicity after topical application.* Skin pharmacology and physiology, 2005. **18**(4): p. 170-174.
87. Cabrera, M., et al., *Synthetic chalcones, flavanones, and flavones as antitumoral agents: Biological evaluation and structure–activity relationships.* Bioorganic & Medicinal Chemistry, 2007. **15**(10): p. 3356-3367.
88. IMMUNOSENSORS, P., *Structure of chemical compounds, methods of analysis and process control.* Pharmaceutical Chemistry Journal, 2008. **42**(4).
89. Xu, L., et al., *Advances in the study of oxyresveratrol.* International Journal of Pharmacology, 2014. **10**(1): p. 44-54.
90. Shibata, M.-A., et al., *α-Mangostin extracted from the pericarp of the mangosteen (Garcinia mangostana Linn) reduces tumor growth and lymph node metastasis in an immunocompetent xenograft model of metastatic mammary cancer carrying a p53 mutation.* BMC medicine, 2011. **9**(1): p. 69.
91. Kumar, D., *Isolation, synthesis and pharmacological evaluation of some novel curcumin derivatives as anticancer agents.* Journal of Medicinal Plants Research, 2012. **6**(14): p. 2880-2884.
92. Lahmer, N., et al., *Hesperidin and hesperitin preparation and purification from Citrus sinensis peels.* Der PharmaChemica, 2015. **7**(2): p. 1-4.
93. Boonnoun, P., et al., *Purification of free lutein from marigold flowers by liquid chromatography.* Engineering Journal, 2012. **16**(5).
94. Kumar, R., et al., *Improvement of the isolation and purification of lutein from marigold flower (Tagetes erecta L.) and its antioxidant activity.* Journal of food process engineering, 2010. **33**(6): p. 1065-1078.
95. Tiew, P., et al., *Coumarins from the heartwoods of Mansonia gagei Drumm.* Phytochemistry, 2002. **60**(8): p. 773-776.
96. Saha, K., H. Seal, and M. Noor, *Isolation and characterization of piperine from the fruits of black pepper (Piper nigrum).* Journal of the Bangladesh Agricultural University, 2014. **11**(1): p. 11-16.
97. Singh, R.K., et al., *The patient's guide to Psoriasis Treatment. Part 1: UVB phototherapy.* Dermatology and therapy, 2016. **6**(3): p. 307-313.

APPENDIX

Appendix A

UV absorbance of natural products

UV-A and –B absorber agents were measured the UV absorbance at the concentration 0.01, 0.005, 0.0025, 0.0001% w/v which were performed in **Table A1-9**

Table A1 The UV absorbance of quercetin hydrate **(4).**

Compound (%w/v)	λ max		Absorbance at 311 nm (a.u.)	Absorber type
	nm	Absorbance (a.u.)		
0.01	370	6.0651	2.148	UV-A
0.005	370	2.9996	1.0889	UV-A
0.0025	380	1.4231	0.5235	UV-A
0.001	380	0.503	0.2315	UV-A

Table A2 The UV absorbance of oxyresveratrol **(12).**

Compound (%w/v)	λ max		Absorbance at 311 nm (a.u.)	Absorber type
	nm	Absorbance (a.u.)		
0.01	330	5.2242	3.0280	UV-A
0.005	330	3.9333	2.5942	UV-A
0.0025	330	2.1306	1.3561	UV-A
0.001	330	1.7100	0.8210	UV-A

Table A3 The UV absorbance of curcumin **(14).**

Compound (%w/v)	λ max		Absorbance at 311 nm (a.u.)	Absorber type
	nm	Absorbance (a.u.)		
0.01	360	4.9673	2.8716	UV-A
0.005	360	3.9916	1.6813	UV-A
0.0025	380	3.1263	0.9890	UV-A
0.001	380	1.7213	0.4352	UV-A

Table A4 The UV absorbance of catechin **(6).**

Compound (%w/v)	λ max		Absorbance at 311 nm (a.u.)	Absorber type
	nm	Absorbance (a.u.)		
0.01	280	1.5585	0.0496	UV-B
0.005	280	0.5666	0.0347	UV-B
0.0025	280	0.2058	0.0193	UV-B
0.001	280	0.0622	0.0085	UV-B

Table A5 The UV absorbance of naringenin **(3)**.

Compound (%w/v)	λ max		Absorbance at 311 nm (a.u.)	Absorber type
	nm	Absorbance (a.u.)		
0.01	280	4	2.5524	UV-B
0.005	290	3.6722	1.3507	UV-B
0.0025	290	1.9941	0.7075	UV-B
0.001	290	0.8397	0.3062	UV-B

Table A6 UV absorbance of hesperetin **(18).**

Compound (%w/v)	λ max		Absorbance at 311 nm (a.u.)	Absorber type
	nm	Absorbance (a.u.)		
0.01	290	3.5129	1.1645	UV-B
0.005	290	1.9918	0.5851	UV-B
0.0025	290	0.9931	0.3158	UV-B
0.001	280	0.5548	0.1582	UV-B

Table A7 The UV absorbance of lutein **(19).**

Compound (%w/v)	λ max		Absorbance at 311 nm (a.u.)	Absorber type
	nm	Absorbance (a.u.)		
0.01	400	3.5084	0.7816	UV-B
0.005	400	2.3184	0.2665	UV-B
0.0025	400	0.7682	0.0876	UV-B
0.001	400	0.2221	0.0267	UV-B

Table A8 The UV absorbance of berberine chloride hydrate **(2).**

Compound (%w/v)	λ max		Absorbance at 311 nm (a.u.)	Absorber type
	nm	Absorbance (a.u.)		
0.01	280	4	2.0186	UV-A &-B
0.005	340	3.2601	1.1401	UV-A &-B
0.0025	350	1.9975	0.6356	UV-A &-B
0.001	350	0.8384	0.2782	UV-A &-B

Table A9 The UV absorbance of demethoxycurcumin **(15).**

Compound (%w/v)	λ max		Absorbance at 311 nm (a.u.)	Absorber type
	nm	Absorbance (a.u.)		
0.01	280	3.4065	1.5326	UV-A&-B
0.005	280	2.7212	1.0218	UV-A&-B
0.0025	280	1.4816	0.5453	UV-A&-B
0.001	280	1.0522	0.3452	UV-A&-B

Table A10 The UV absorbance of mansonone G **(20).**

Compound (%w/v)	λ max		Absorbance at 311 nm (a.u.)	Absorber type
	nm	Absorbance (a.u.)		
0.01	400	3.8362	0.3306	UV-A&-B
0.005	280	3.0523	0.2136	UV-A&-B
0.0025	280	1.7092	0.1222	UV-A&-B
0.001	280	0.7355	0.0741	UV-A&-B

Appendix B

Photostability

The calibration curve of UV absorbance from quercetin hydrate **(4)** and mansonone G **(20)** at the concentration 0.001, 0.0025, 0.0050, 0.0100 %w/v were shown in **Figure B1-2.**

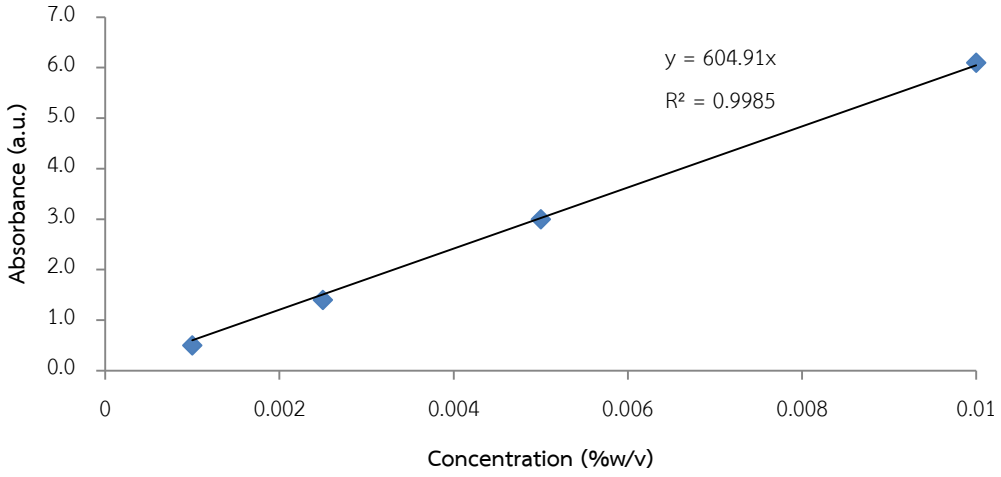

Figure B1 The calibration curve of UV absorbance from quercetin hydrate **(4).**

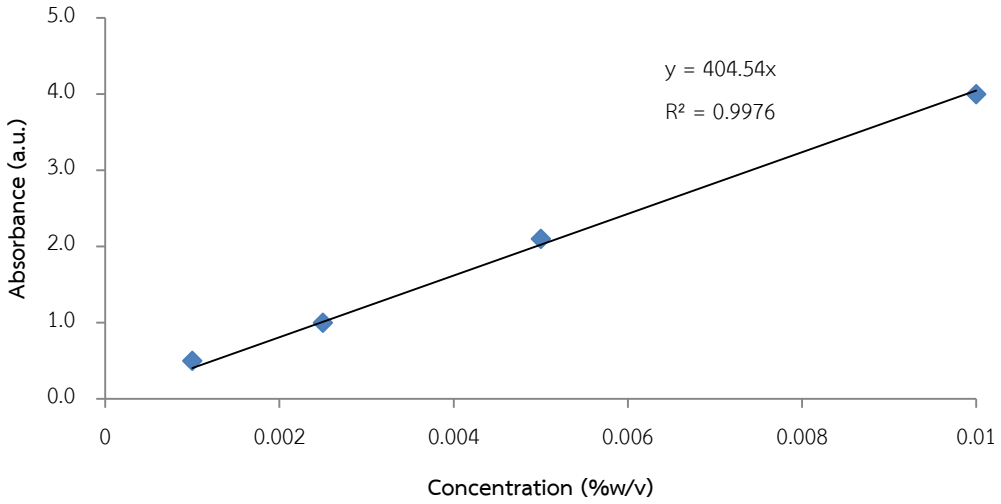

Figure B2 The calibration curve of UV absorbance from mansonone G **(20).**

VITA

Ms. Sruangsuda Mawaha was born on October 31, 1992 in Ratchaburi province, Thailand. She graduated with Degree of Bachelor of Science (Chemistry) from Faculty of Science, King Mongkut's University of technology Thonburi, in 2014. She graduated a Master Degree of Science in Biotechnology in 2017 from program in Biotechnology, Faculty of Science, Chulalongkorn University, Bangkok, Thailand. She presented poster at ASTC 2017.